ACS APPLIED MATERIALS & INTERFACES

Research Article

Cite This: ACS Appl. Mater. Interfaces 2019, 11, 12283−12297

www.acsami.org

Pectin Methacrylate (PEMA) and Gelatin-Based Hydrogels for Cell Delivery: Converting Waste Materials into Biomaterials

Mehdi Mehrali,[†] Ashish Thakur,[†] Firoz Babu Kadumudi,[†] Malgorzata Karolina Pierchala,[†] Julio Alvin Vacacela Cordova,[†,‡] Mohammad-Ali Shahbazi,[†] Mohammad Mehrali,[§] Cristian Pablo Pennisi,[‡] Gorka Orive,[∥,⊥,#,▽] Akhilesh K. Gaharwar,[○,◆,¶] and Alireza Dolatshahi-Pirouz*[,†,⋈]

[†]Department of Health Technology, Center for Intestinal Absorption and Transport of Biopharmaceuticals, Technical University of Denmark, 2800 Kgs. Lyngby, Denmark

[‡]Department of Health Science and Technology, Laboratory for Stem Cell Research, Aalborg University, Fredrik Bajers Vej 3B, 9220, Aalborg, Denmark

[§]Faculty of Engineering Technology, Laboratory of Thermal Engineering, University of Twente, Enschede 7500 AE, The Netherlands

[∥]NanoBioCel Group, Laboratory of Pharmaceutics, School of Pharmacy, University of the Basque Country UPV/EHU, Paseo de la Universidad 7, 01006 Vitoria-Gasteiz, Spain

[⊥]Biomedical Research Networking Centre in Bioengineering, Biomaterials and Nanomedicine (CIBER-BBN), 01006 Vitoria-Gasteiz, Spain

[#]University Institute for Regenerative Medicine and Oral Implantology-UIRMI (UPV/EHU-Fundacion Eduardo Anitua), 01007 Vitoria, Spain

[▽]Singapore Eye Research Institute, The Academia, 20 College Road, Discovery Tower, 169856 Singapore

[○]Department of Biomedical Engineering, [◆]Department of Materials Science and Engineering, and [¶]Center for Remote Health Technologies and Systems, Texas A&M University, College Station, Texas 77843, United States

[⋈]Department of Regenerative Biomaterials, Radboud University Medical Center, Philips van Leydenlaan 25, Nijmegen 6525 EX, The Netherlands

Supporting Information

ABSTRACT: The emergence of nontoxic, eco-friendly, and biocompatible polymers derived from natural sources has added a new and exciting dimension to the development of low-cost and scalable biomaterials for tissue engineering applications. Here, we have developed a mechanically strong and durable hydrogel composed of an eco-friendly biopolymer that exists within the cell walls of fruits and plants. Its trade name is pectin, and it bears many similarities with natural polysaccharides in the native extracellular matrix. Specifically, we have employed a new pathway to transform pectin into a ultraviolet (UV)-cross-linkable pectin methacrylate (PEMA) polymer. To endow this hydrogel matrix with cell differentiation and cell spreading properties, we have also incorporated thiolated gelatin into the system. Notably, we were able to fine-tune the compressive modulus of this hydrogel in the range ∼0.5 to ∼24 kPa: advantageously, our results demonstrated that the hydrogels can support growth and viability for a wide range of three-dimensionally (3D) encapsulated cells that include muscle progenitor (C2C12), neural progenitor (PC12), and human mesenchymal stem cells (hMSCs). Our results also indicate that PEMA-gelatin-encapsulated hMSCs can facilitate the formation of bonelike apatite after 5 weeks in culture. Finally, we have demonstrated that PEMA-gelatin can yield micropatterned cell-laden 3D constructs through UV light-assisted lithography. The simplicity, scalability, processability, tunability, bioactivity, and low-cost features of this new hydrogel system highlight its potential as a stem cell carrier that is capable of bridging the gap between clinic and laboratory.

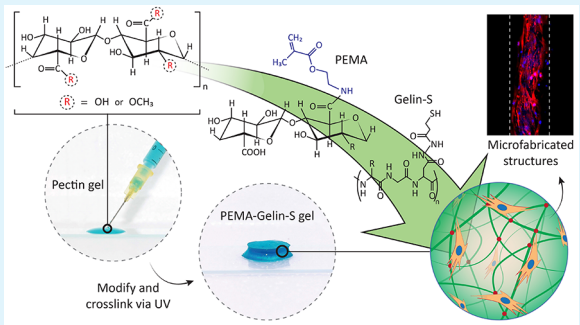

KEYWORDS: *tissue engineering, polysaccharide, hydrogel, pectin, gelatin, human mesenchymal stem cells, muscle, neural, bone*

INTRODUCTION

In the current aging population, degenerative diseases caused by compromised tissues have become one of the major healthcare

Received: January 3, 2019
Accepted: March 13, 2019
Published: March 13, 2019

DOI: 10.1021/acsami.9b00154
ACS Appl. Mater. Interfaces 2019, 11, 12283−12297

challenges worldwide.[1] A promising avenue to address this looming challenge entails the delivery of regenerative cells to the affected tissues.[2] In response, tissue engineers have proposed the development of three-dimensional (3D) microenvironments that can guide embedded cells into mature tissue, which can integrate in vivo with dysfunctional tissues for repair.[2−7] The underscored importance of such 3D systems has led to the conception of hydrogel-based biomaterials.[8] These systems can shield cells from the detrimental shear forces throughout the needle injection phase to maximize postinjection cell viability and, at the same time, can retain the cells within a 3D environment to enable optimal tissue regeneration.[9,10]

Put simply, hydrogels are largely hydrated 3D structures stabilized via cross-linked hydrophilic polymers; their aqueous characteristics enable a native-like state for the encapsulated cells.[11,12] The multifaceted challenge in tissue engineering is to find an ideal hydrogel pre-polymer that can mimic the biology of human tissues in terms of structure, function, and performance.[7,12,13] Furthermore, these polymers are also idealized to be conveniently functionalized so that their chemical and physical behavior can be manipulated for therapeutics such as stem cell and drug delivery.[14−17] Biopolymers derived from natural sources such as collagen, elastin, hyaluronic acid, and heparin are appealing in this respect because they are biocompatible, biodegradable, and are easy to modify with various cell adhesive and differentiation promoting motifs.[18−22] Alternatively, other approaches that are based on synthetic materials such as poly(ethylene glycol) and cell adhesive oligopeptides among others have also been explored over the years.[17,23,24] However, even though they are biocompatible and easier to modify chemically and biocompatible as well, they are typically more costly and less scalable than naturally derived biomaterials.[21,25] Therefore, natural biopolymers are the ones that currently hold most promise as tissue engineering hydrogels, as they are nontoxic, biocompatible, easily accessible, and inexpensive at the same time. Indeed, some of these hydrogels, particularly the alginate- and gelatin-based ones, have been FDA-approved and are already a utility in the clinic.[26,27] Still, alginate-based hydrogels are usually associated with brittleness and low mechanical stability,[28] while the gelatin-based ones tend to degrade rapidly within the body—since they form the substrate for collagenase.[26] For these reasons, the quest for a suitable polymeric source remains one of the critical challenges in the field of hydrogel-based tissue engineering.

Here, we have addressed some of the aforementioned shortcomings that currently dominate the field by using cheap and readily available waste materials to manufacture a low-cost and biocompatible hydrogel system. To this end, we have primarily used pectin, an inexpensive and negatively charged polysaccharide that is found in the cell walls of terrestrial plants.[29−31] Because of pectins thickening and gelling abilities, it has been widely employed in the food processing industry.[32,33] The same properties have made it a suitable biomaterial-based carrier for drug delivery and gene delivery.[34,35] In recent years, it has also received increasing attention from tissue engineers because it is easy to cross-link and is biodegradable, nontoxic, and biocompatible.[31,36−40] However, despite its resemblance with many of the sugar-like biopolymers (hyaluronic acid, alginate, carrageenan, etc.) used in tissue engineering, pectin is still not a well-established biopolymer in the field.[41]

In this study, we have compensated for this "lack of attention" by developing a feasible methodology for methacrylating pectin into pectin methacrylate (PEMA) and demonstrated that this approach can be used to manufacture mechanically stable cell culture systems. This methodology can also (using ultraviolet (UV) light-assisted lithography) enable a cell-laden hydrogel that resembles the complex tissue-like architectures present in the human body.

Advantageously, we have demonstrated that PEMA-based hydrogels enable a sustained viability for a wide range of cells (muscle (C2C12), neural progenitor (PC12), and human mesenchymal stem cells (hMSCs)) for long periods of time. Notably, our system exhibits superior mechanical and load-bearing properties than many of the brittle hydrogels currently used in the clinic and in combination with another waste material, namely, gelatin from slaughterhouse waste, pectin, could facilitate cell growth and spreading in 3D (Figure 1). It also displays a favorable long-term degradation profile and enables hMSCs to exhibit important bone differentiation markers. Indeed, PEMA-gelatin can stimulate hMSCs to secrete a mineralized bone matrix with hydroxyapatite (HA)-like properties, one of the most important mineral components of bone.[42−46] It therefore holds great promise as a carrier system for treating bone disorders through targeted stem cell delivery. To date, several studies have successfully used hydrogels for various tissue engineering applications; however, only a few of them encompass the wide range of properties required of commercializable and clinically implementable tissue engineering hydrogels.

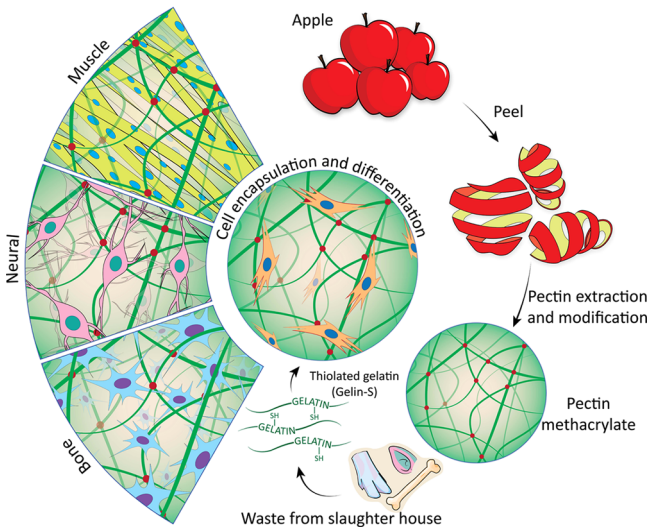

Figure 1. Pectin from apple waste and gelatin from slaughterhouse waste were combined into a potent hydrogel for three-dimensional (3D) cell encapsulation and differentiation.

RESULTS

Commercially available pectin is chemically defined as an α-(1−4)-linked D-galacturonic acid polysaccharide that is partially methyl esterified (Figure 2a).[30] It therefore contains a mixture of carboxyl groups and methoxyl groups. Here, we have activated its carboxyl groups with 1-ethyl-3-(3-dimethylaminopropyl)-carbodiimide (EDC) and *N*-hydroxysuccinimide (NHS) to functionalize its polymeric backbone with methacrylate groups (Figure 2a) to obtain pectin methacrylate (PEMA), a photo-cross-linkable polymer that can transform into a hydrogel with low-level UV light and a suitable photoinitiator (PI) (Figure 2b). Additionally, we also incorporated thiolated gelatin (Gelin-S)

DOI: 10.1021/acsami.9b00154
ACS Appl. Mater. Interfaces 2019, 11, 12283−12297

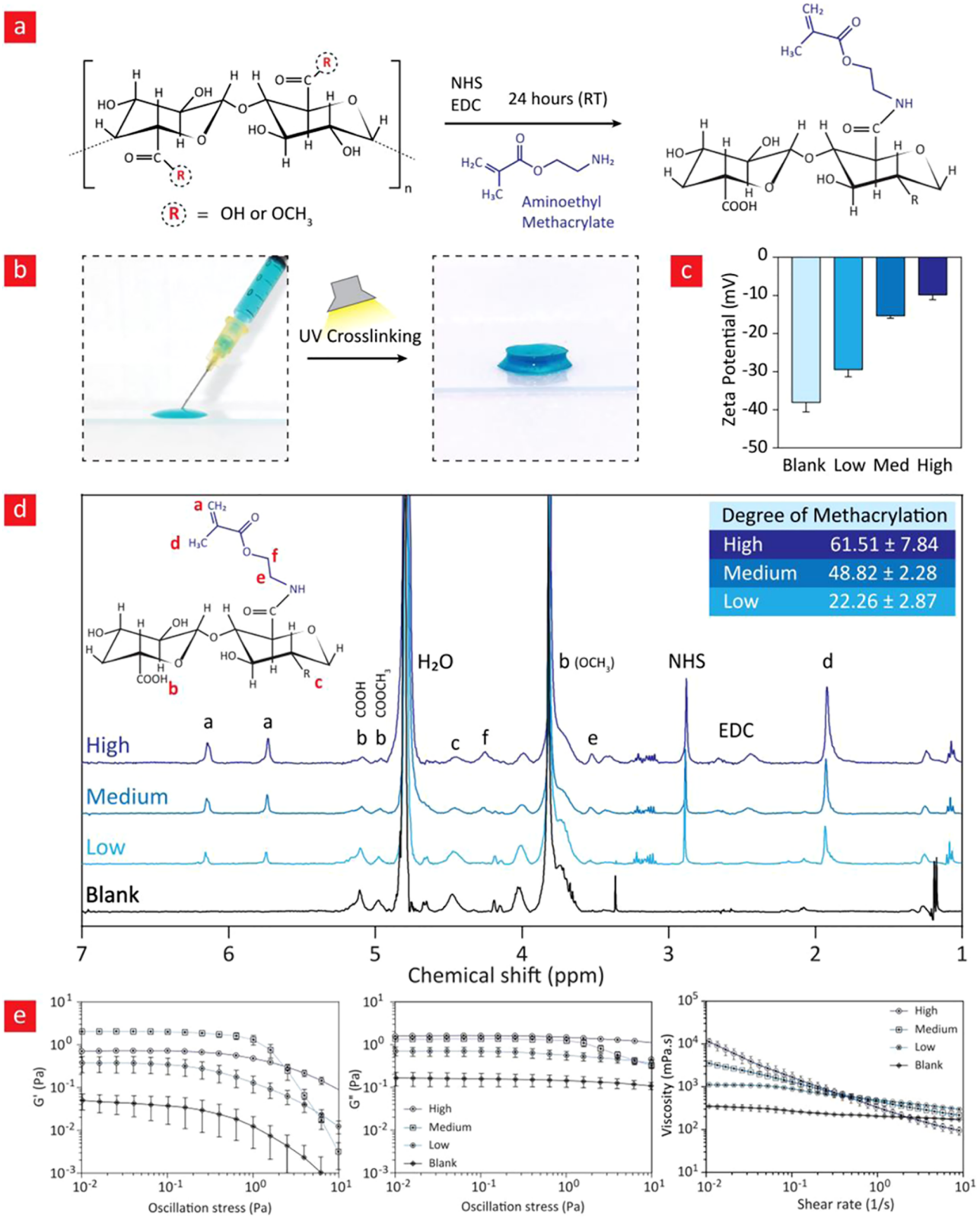

Figure 2. Chemistry behind the developed hydrogels and the corresponding characterizations. (a) Chemical structure of pectin before and after methacrylation. (b) Photographic images of PEMA before and after UV cross-linking. (c) ζ potential measurements of PEMA with low, medium (Med), and high methacrylation degrees. (d) Nuclear magnetic resonance (NMR) spectroscopy of PEMA with different methacrylation degrees. (e) Rheological analysis of the different PEMA variants.

into the system using a Michael addition reaction between thiol and acrylate groups. This inclusion significantly increased the bioactivity of the composite scaffold while enhancing its mechanical properties simultaneously. We have characterized this hydrogel in terms of its chemical, mechanical, hydration, and morphological properties in the following sections. In

DOI: 10.1021/acsami.9b00154
ACS Appl. Mater. Interfaces 2019, 11, 12283−12297

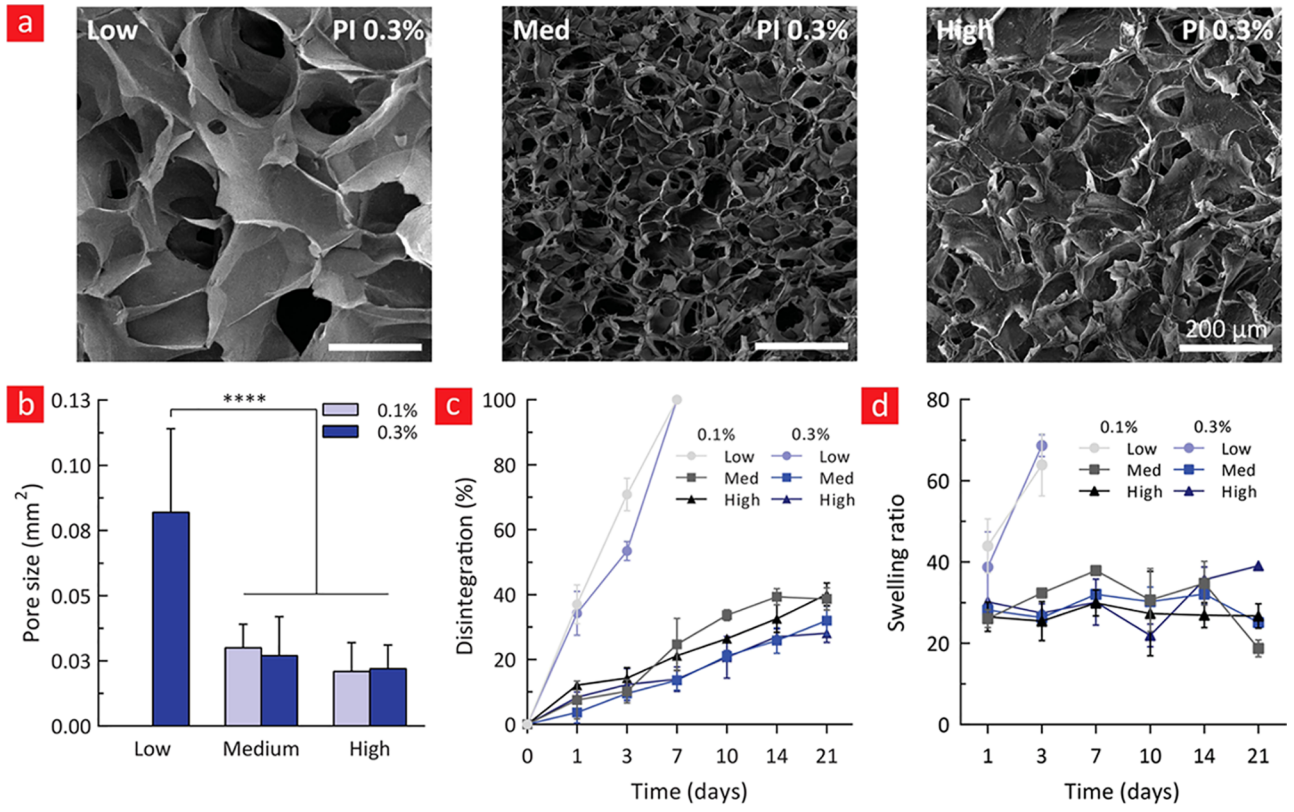

Figure 3. Morphological and stability assays. (a) Scanning electron microscopy (SEM) of the different hydrogel variants developed herein. (b) Pore sizes within the imaged hydrogels were analyzed with ImageJ and are displayed. (c) Disintegration and (d) swelling profile of PEMA hydrogels with different methacrylation degrees and photoinitiator concentrations.

addition, we have also thoroughly examined its structural integrity and degradation profile and demonstrated that it can sustain the viability of a wide range of cell types for up to 21 days in culture.

Chemical Characterization. In brief, the carboxyl groups on the backbone of pectin were activated with NHS/EDC and conjugated with aminoethyl methacrylate to yield PEMA prepolymers (Figure 2a). PEMA polymers can be readily cross-linked to form a hydrogel by UV exposure in the presence of a photoinitiator (Irgacure 2959) (Figure 2b). Specifically, the ζ potential analysis of PEMA (Figure 2c) reveals a correlation between its methacrylation degree and its charge, the charge becoming more positive as the methacrylation degree increases (0 → 60%). This increased potential can be attributed to a reduced number of negatively charged carboxyl groups and, therefore, an overall increase of the charge of PEMA, which is indicative of a successful functionalization.[47]

The functionalization of pectin with methacrylate groups was further validated using nuclear magnetic resonance (NMR) spectroscopy (Figure 2d). The singlet peaks at ~5.1 and ~4.9 ppm of pure pectin proton nuclear magnetic resonance (^{1}H NMR) are assigned to the methyl carboxylate ($COOCH_3$) and carboxylic acid (COOH) groups, respectively (denoted as R, Figure 2a).[48,49] Aminoethyl methacrylate conjugates to these $COOCH_3$ or COOH groups, and thus upon methacrylation, the corresponding signals at ~5.1 and ~4.9 ppm were gradually decreased. This methacrylation was further confirmed from the ^{1}H NMR spectra via the presence of methacrylate peaks at ~5.7, ~6.1, ~4.2, ~3.7, and ~1.9 ppm (Figure 2d).[50,51]

Upon UV-mediated cross-linking, the methacrylate-associated NMR signals (~5.7, ~6.1, and ~1.9 ppm) disappeared and new signals at 1.85, 1.36, and 1.12 ppm emerged, validating the formation of a cross-linked product (Figure S1a).[52] The pectin methacrylation and UV-assisted cross-linking were also validated via Fourier transform infrared (FTIR) spectroscopy (Figure S1b). The FTIR spectrum of pure pectin has signals at 1735 and 1612 cm^{-1} corresponding to the carbonyl group (methyl carboxylate and carboxylic acid).[49] After methacrylation, the peak at 1612 cm^{-1} shifts to 1645 cm^{-1} due to an amide bond (amide I) formation between aminoethyl methacrylate and carboxylic acid/methyl carboxylate groups, and the intensity of the peak at 1645 cm^{-1} is increased with increasing degree of methacrylation. In particular, the peak at 1645 cm^{-1} stems from amide I, while the peak at 1544 cm^{-1} corresponds to amide II and that at 806 cm^{-1} to =CH acrylate groups.[53−55] After UV-cross-linking, the amide I peak from PEMA shifts to 1600 cm^{-1} and the acrylate (=CH)-derived signal disappears.[56,57] Furthermore, FTIR spectroscopy was also used to characterize the interaction of Gelin-S after UV-cross-linking with PEMA. From these spectra, we observed a thiol-Michael addition reaction between thiolated gelatin (Gelin-S) and the methacrylate groups present on PEMA, which is evident from the disappearance of the acrylate associated at 806 cm^{-1} and the thiol group at 2450 cm^{-1} due to the reaction between thiol and the acrylate groups (Figure S1b).[55]

Moreover, our rheology data confirmed the above-mentioned chemical modifications of PEMA, as the storage/loss modulus and viscosity of the prepolymer solution was generally higher for PEMA-High and PEMA-Med compared to PEMA-Low and PEMA-Blank (Figure 2e). This can be attributed to the methacrylate groups as they are capable of hydrophobic interaction, which in turn can result in some gelling behavior;

DOI: 10.1021/acsami.9b00154
ACS Appl. Mater. Interfaces 2019, 11, 12283−12297

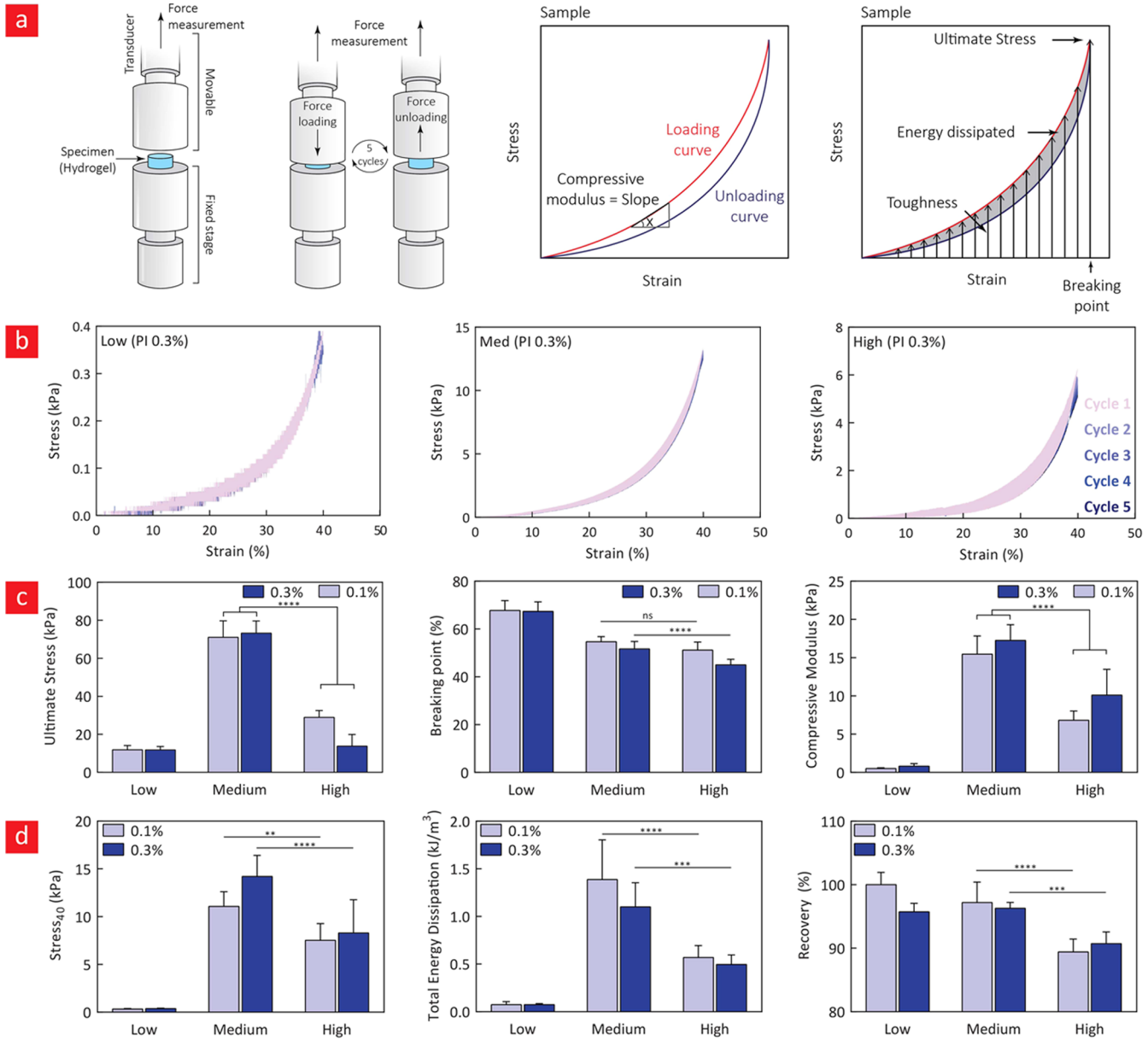

Figure 4. Mechanical analysis. (a) Brief explanation of the working principle behind the mechanical analysis. (b) Cyclic stress−strain curves (up to five cycles) corresponding to PEMA hydrogels cross-linked in the presence of 0.3% photoinitiator. (c) Ultimate stress, strain at breaking point and compressive modulus of the respective hydrogels. (d) Stress at 40% strain, total energy dissipated, and mechanical recovery after 40% strain were retrieved from the stress−strain curves. The significant differences between different data sets were determined through one-way analysis of variance (ANOVA), followed by Tukey's post hoc test. Significance levels are indicated according to the legend: **($p < 0.01$), ***($p < 0.001$), ****($p < 0.0001$), and ns means not significant.

this is also corroborated by the increased positive charge observed from the ζ potential measurements (Figure 2c) of PEMA. Furthermore, we observe a decreasing viscosity upon increasing shear rate (Figure 2a), which is a key feature of shear-thinning systems.

Hydrogel Porosity, Swelling, and Disintegration Studies. An ideal hydrogel carrier should enable cell survival, proliferation, and differentiation, to become amenable for tissue engineering.[5] This function is only possible if the system permits a continuous inflow of nutrients and outflow of metabolic waste products. For this reason, an interconnected hydrogel network with controlled porosity and pore size plays a key role in keeping the encapsulated cells thriving and alive. In this regard, studies have shown that a pore size >100 μm is typically needed to assure that an efficient waste and nutrient exchange occurs with the surrounding environment.[58,59] Scanning electron micrographs of PEMA hydrogels show that the low methacrylation of pectin results in pore areas around 0.08 mm^2, which decrease to ~0.03 mm^2 for PEMA-Med and PEMA-High (Figure 3a), suggesting that our hydrogels are optimal for nutrient and waste exchange.

Next, the hydrogel disintegration and swelling profiles were examined to determine the stability of PEMA (Figure 3c,d). We found that PEMA-Low was unstable and completely disintegrated after 3 days in culture, whereas other PEMA variants remained stable for up to 21 days in culture. We noted that the stability of these systems could be further improved by increasing the photoinitiator concentration from 0.1 to 0.3%.

DOI: 10.1021/acsami.9b00154
ACS Appl. Mater. Interfaces 2019, 11, 12283−12297

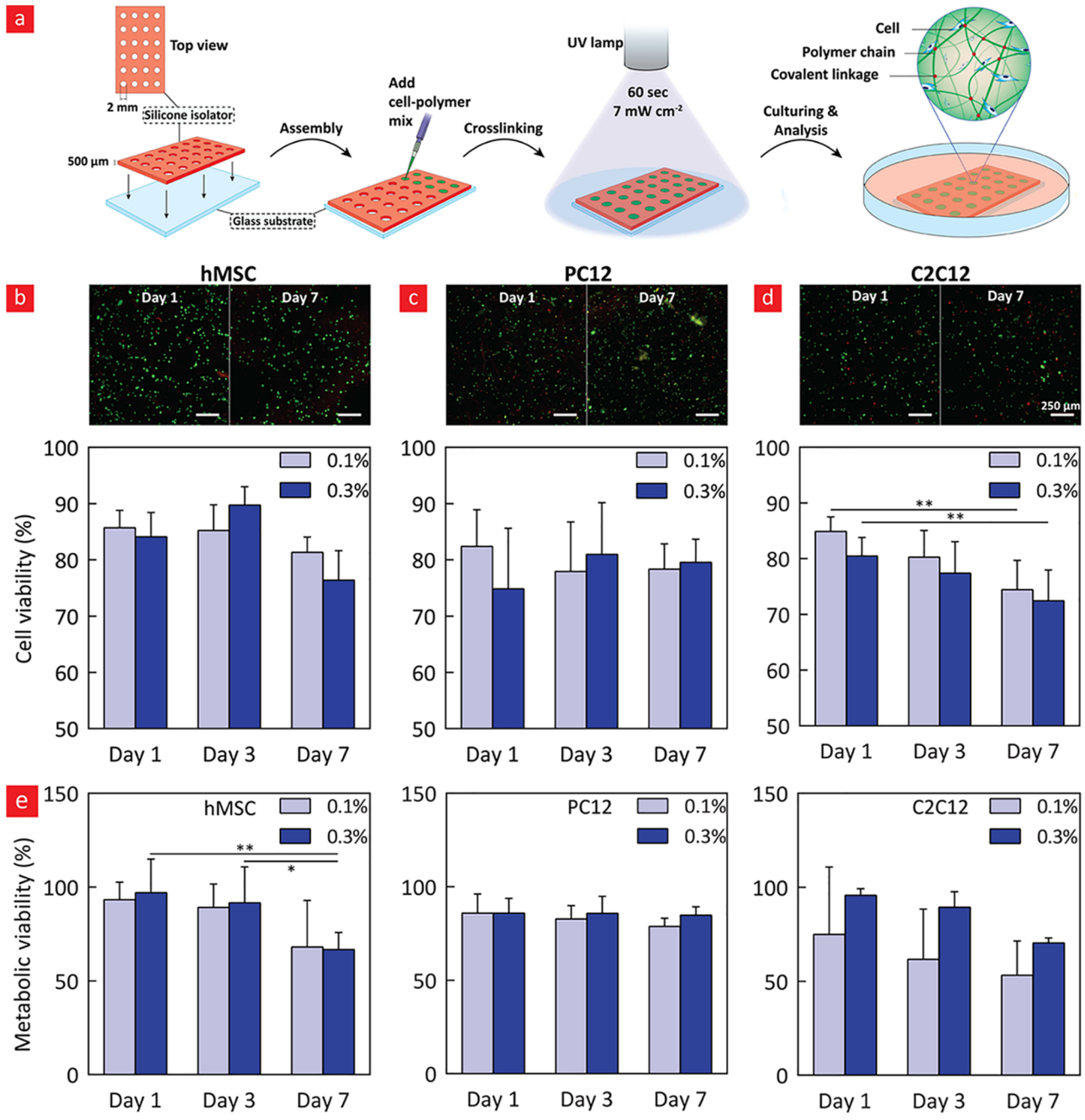

Figure 5. Cell viability studies. (a) Schematic briefly explaining the setup used in the cell-laden hydrogel experiments. (b–d) Viability was determined from live-dead fluorescence imaging (green corresponds to live cells and red to dead cells), from which the number of dead, live, and total cells were determined and combined into a cell viability percentage (%). (e) Metabolic viability was likewise determined through a colorimetric assay.

In addition, no change was observed in the water retention capacity of PEMA-Med and PEMA-High, as they remained at a swelling factor of ∼30 for up to 21 days in culture (Figure 3d).

In summary, the results displayed in Figure 3b suggest that PEMA-Low is not suitable for long-term cell culture because it disintegrates rapidly, whereas PEMA-Med and PEMA-High display an optimal pore size and long-term physiological stability.

Mechanical Analysis. The mechanical properties of a tissue engineering hydrogel play an important role in directing the stem cell differentiation into a specific lineage. For instance, studies have shown that a Young's modulus in the range of 25–60 kPa is typically needed to support optimal osteogenesis, while typical moduli for supporting differentiation into neural and muscle lineages are 8–17 and 0.1–1 kPa, respectively.[60,61] Since most of the tissues in the human body are very dynamic, a hydrogel carrier for stem cell delivery should be able to also endure continual and cyclic mechanical forces.

To characterize the mechanical properties of our hydrogels, we examined their stress–strain curves both with and without cyclic loading (five cycles) (Figure 4a). This allowed us to determine the compressive modulus, durability, material toughness, and the amount of energy dissipated per cycle. As seen in Figure 4b, the mechanical hysteresis after each cyclic loading was low for PEMA-Low and PEMA-Med, while it was slightly more pronounced for PEMA-High. This demonstrates

DOI: 10.1021/acsami.9b00154
ACS Appl. Mater. Interfaces 2019, 11, 12283–12297

the elastic nature of PEMA hydrogels, and for this reason, they should be able to readily integrate into load-bearing environments such as cartilage, muscle, and bone, unlike their brittle and less elastic alternatives that are currently used in the clinic (alginate, gelatin, etc.). For example, the compressive modulus of 5% (w/v) gelatin methacrylate (GelMA) hydrogels with ∼80% methacrylation degree has been reported in the range of ∼3−5 kPa for experiments dealing with sustainable cell encapsulation.[62] Additionally, the compressive modulus of alginate methacrylate (2% (w/v)) has been reported to be ∼4−5 kPa.[63]

We further characterized the mechanical properties of different variants of PEMA and found that the compressive modulus, ultimate stress, and total energy dissipated were the highest for PEMA-Med. We attribute this high energy dissipation for PEMA-Med to arise from its manifold larger ultimate stress and compressive modulus compared to PEMA-Low and PEMA-High. The PEMA-Med system also recovered nearly 100% after continuous mechanical loadings (difference in ultimate stress between cycles 2 and 3), while the recovery remained substantially lower for PEMA-High at around 90% (cycle 2 → 5). The compressive modulus of the hydrogels could be further varied from ∼0.5 to ∼17 kPa, and by including Gelin-S into PEMA-Med, the compressive modulus increased to ∼24 kPa, with a hydrogel breaking point of ∼62% (Figure S3), while the mechanical recovery remained >90% (cycle 2 → 5). For these reasons, the developed PEMA-gelatin can potentially be fine-tuned to meet the required mechanical properties for an optimal guidance of stem cells into muscle, neural, or bone tissue. However, PEMA-High was found to be highly hydrophobic, requiring excessive agitation for optimal dissolution, and PEMA-Low was highly unstable under physiological conditions (Figure 3c,d); therefore, we limit our studies to PEMA-Med hydrogels.

Cell Viability. Cell viabilities of encapsulated hMSC, PC12, and C2C12 cells were evaluated for up to 7 days in culture by using a live-dead staining kit and a colorimetric assay. The images of the live-dead stained hydrogels are shown in Figure 5b−d, from which the cell viability was quantified by counting the number of dead cells (red) and live cells (green), and therefrom calculating the percentage of live cells (viability %). The cell viability was around 80−85% for 3 days in culture, after which it dropped below 80%. As supporting data, we performed a series of colorimetric assays that, to a large extent, followed the same trends as the live-dead images (Figure 5e). The viability results displayed in Figure 5b−e are in accordance with the current FDA guidelines for clinical approval of stem cell therapies, which mandates a 70% stem cell viability.[64]

To increase the biocompatibility of PEMA hydrogels, we incorporated another biopolymer into this system—thiolated gelatin (Gelin-S)—that can form covalent bonds through a Michael addition reaction with the acrylate groups on PEMA.[65] The spreading and cell viability of hMSCs within this system were found to be higher than pristine PEMA; this emphasizes the importance of a combination of polysaccharide and a collagen-like backbone in tissue engineering hydrogels. Our results show that the hMSCs could reach ∼50% confluency with ∼90% survival after 14 days in 3D culture (Figure 6). The modified PEMA hydrogel was found to be stable for 21 days in culture and enabled the cells to form well-defined actin fibers (Figure S4a).

Osteogenic Differentiation. Some of the most important hallmarks of osteogenic differentiation are alkaline phophatase (ALP) secretion and extracellular matrix (ECM) mineralization. The two are interconnected as ALP is an early bone marker protein in the process of bone calcification. In this process, ALP plays an important role because it is capable of hydrolyzing pyrophosphate—an inhibitor of mineralization—into inorganic phosphate, a calcification promoter.[66] For these reasons, an ALP assay was employed and from this assay, we observed a high alkaline phosphatase (ALP) secretion from the hMSCs after 7 days in culture, suggesting that PEMA-gelatin is amenable as a stem cell carrier for targeting bone disorders (Figure S4b). We

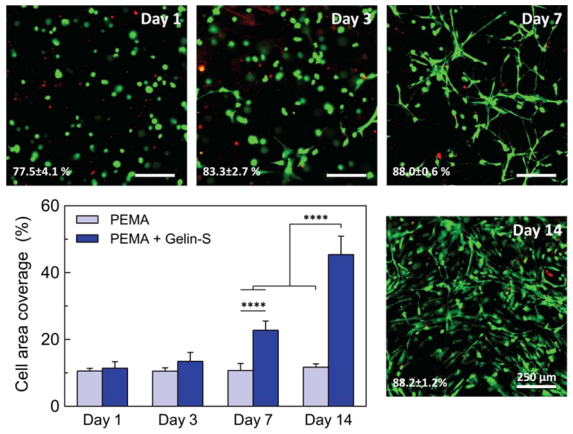

Figure 6. hMSCs spreading and viability within PEMA-gelatin. In brief, cells were encapsulated and live-dead fluorescence imaged on days 1, 3, 7, and 14. The images showed cell viability at around 80%, which increased to around 90% after 14 days in culture. The cell area coverage was likewise quantified from the live-dead fluorescence images.

have also examined the formation of calcium deposits through Alizarin Red S (ARED) staining, as ARED displays strong affinity for calcium (Figure 7a). These results clearly show significant ARED staining for hMSCs-laden PEMA-gelatin hydrogels cultured in osteogenic media after 5 weeks in culture. Unfortunately, control samples cultured in normal growth media started to degrade after 5 weeks and it was thus not possible to include these here.

We took our calcification assays a step further by using scanning electron microscopy (SEM) to put the apatite-inducing capacity of the hydrogels in the spotlight (Figure 7b). The SEM images clearly show that the hydrogels were completely densified after 5 weeks in culture compared to our porous pristine hydrogels (Figure 3a). To elucidate the cause of this interesting phenomenon, we turned to energy-dispersive X-ray (EDAX) spectroscopy (Figure 7c,d). From the EDAX measurements, it is evident that the main ingredients in the observed dense deposits in Figure 7b are indeed calcium and phosphate, two of the main components of bone apatite. Furthermore, we also observed small traces of another important bone mineralite, namely, magnesium. Notably, the calcium phosphate ratio was calculated to be 1.68 ± 0.03, which is really close to the one typically reported for hydroxyapatite (HA) (1.67), which is one of the most important components in the hard phase of bone.

Finally, we turned to FTIR and X-ray diffraction (XRD) measurements to characterize the speculated bone apatite formation even more (Figure 7e,f). From the FTIR results, a strong $\upsilon_4(PO_4)^{-3}$ peak was observed in PEMA-gelatin (but not pristine hydrogels) after 5 weeks in culture. This peak is one of the most widely recognized FTIR-based HA markers.[67]

DOI: 10.1021/acsami.9b00154
ACS Appl. Mater. Interfaces 2019, 11, 12283−12297

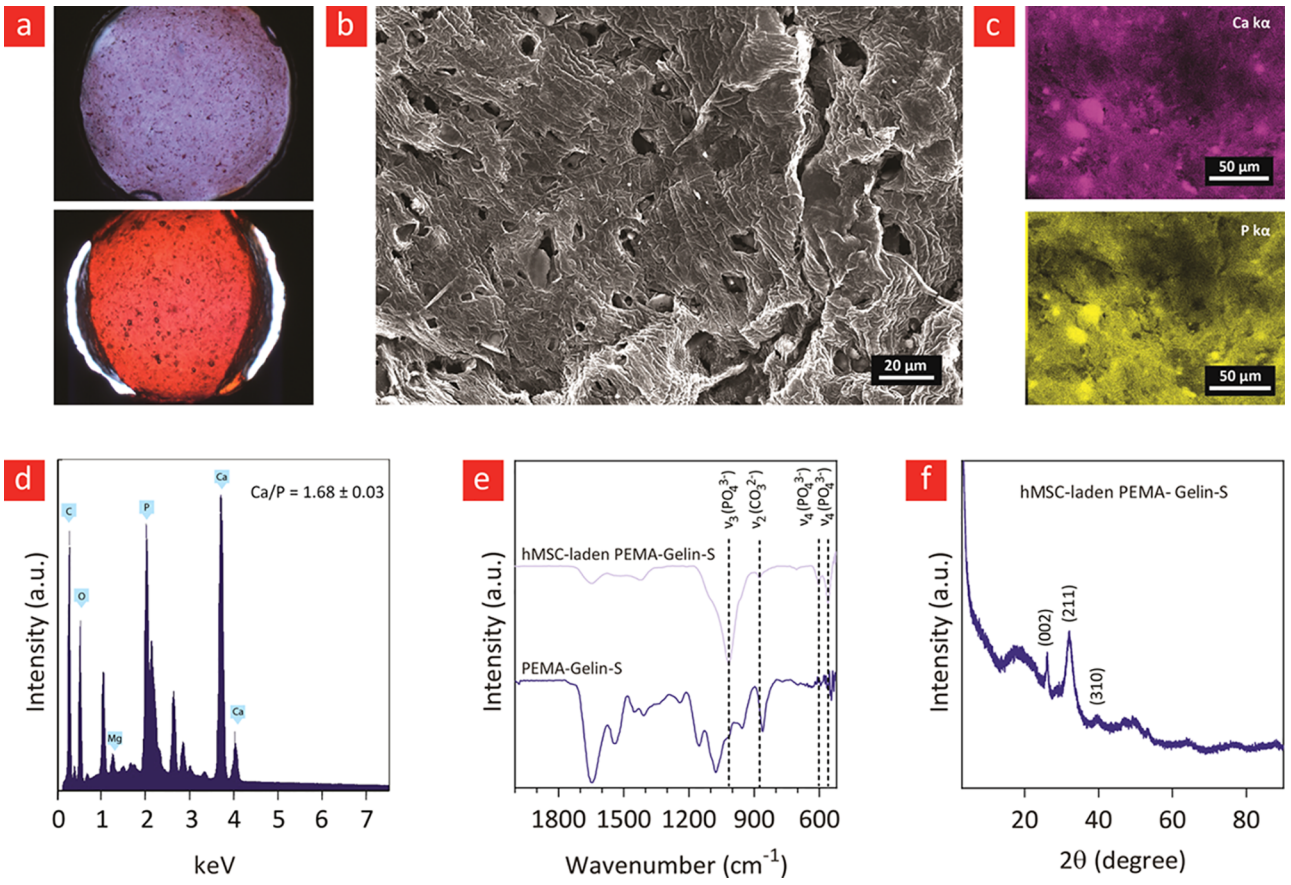

Figure 7. Mineralization studies. (a) Alizarin Red S (ARED) images of hMSC-laden PEMA-gelatin hydrogels after 5 weeks in culture and (b) the associated SEM images. (c) Energy-dispersive X-ray (EDAX) mapping of calcium (purple) and phosphate (yellow) and (d) the associated EDAX spectrum. (e) FTIR and (f) X-ray diffraction (XRD) studies of freeze-dried cell-laden hydrogels following their osteogenic culture.

Similarly, important HA-associated peaks ((002) and (001) crystalline planes) were observed in the XRD results.[68] Overall, the chemical characterizations further support our assumption regarding hMSC-mediated bone apatite formation in PEMA-gelatin.

Microfabrication. The development of well-defined tissue-like architectures is also one of the important challenges in tissue engineering, as tissues such as blood vessels, muscle, cardiac, and bone are characterized by highly anisotropic architectures.[69−71] We have tried to recapitulate this native-like morphology by fabricating micropatterned PEMA-gelatin that consists of microchannels with a spacing and width of 100 μm (Figure 8a). We used a shadow mask and a UV source to cross-link hMSC-laden PEMA-gelatin hydrogels into micropatterned structures. We observed the formation of aligned and highly anisotropic tissue structures with well-defined actin fibers after only 7 days in culture (Figure 8b). These hMSC-based structures remained stable in culture for 21 days and secreted substantial amounts of ALP in differentiation media after 14 days in culture (Figure 8c). Therefore, these results indicate that the developed PEMA-gelatin system could potentially be used as a micropatterned stem cell carrier with the capacity to induce osteogenesis into anisotropic tissue-like structures similar to those found in native spongy bone.

DISCUSSION

Polysaccharide-based biopolymers are among the most widely used materials in biomedical engineering and have unequivocally become the "gold standard" for hydrogels.[21,25,72] One of the primary reasons for the success of polysaccharides in the field is related to their resemblance with the many "sugar-based" polymers in the ECM of native tissues. However, unfortunately, most of these biopolymers are expensive and difficult to functionalize chemically and manufacture in a feasible manner. Among them, the one that has arguable been used the most is alginate because it is readily functionalized, biocompatible, and easy to extract and process for further downstream applications. Indeed, alginate-based hydrogels have already been approved by the U.S. Food and Drug Administration for a number of applications in the clinic.[27] Although alginate exhibits many desirable properties, including nontoxicity, biocompatibility, and the capacity to sustain high cell viability for prolonged periods of time, it still faces a number of shortcomings related to its brittleness and rapid degradation in the body.[28]

Here we have addressed some of these challenges by turning a polysaccharide from apple peel waste, pectin, into a UV-cross-linkable hydrogel with tunable mechanical properties and stability in physiologically relevant environments. Pectin is a low-cost, edible, recyclable, nontoxic, and naturally derived polysaccharide, which makes it appealing for use as a biomaterial.[30] Compared to other natural polymers, established methodologies for transforming pectin prepolymers into tissue engineering hydrogels are rather sparse, making this concept ripe for further investigations. Even still, some methods for cross-linking of pectin have been utilized in recent years to form hydrogels that are biocompatible and stable in physiologically

DOI: 10.1021/acsami.9b00154
ACS Appl. Mater. Interfaces 2019, 11, 12283−12297

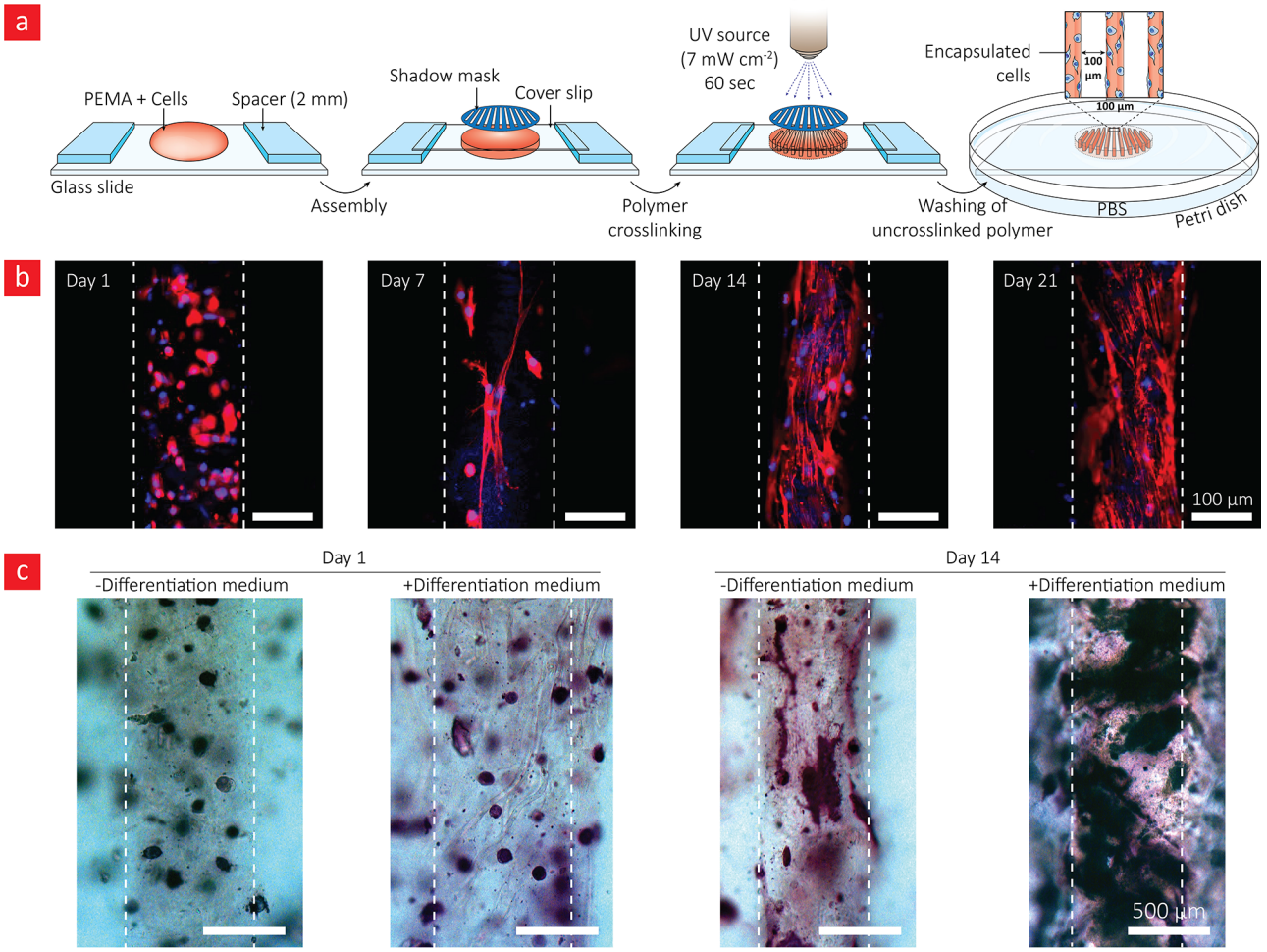

Figure 8. Microfabrication studies. (a) A schematic that briefly explains the setup used to generate cell-laden and microfabricated hydrogels. (b) Phalloidin (red)-Hoechst nuclear staining (blue) of the hydrogels at different time points and (c) alkaline phosphatase staining (purple).

relevant environments.[30,31,36,37,73,74] Many of these methods have been based on electrostatic-driven cross-linking mediated by the interaction of positively charged ions or biopolymers such as chitosan with the negatively charged backbone of pectin.[30,36,37,73,74] Unfortunately, some of the cross-linking ions used in the above-mentioned studies can be toxic for cells at high concentrations, and most ionic cross-linked hydrogels are troubled by brittleness issues, making them unsuitable as regenerative biomaterials for load-bearing tissues. As an alternative, pectin has been recently thiol-norbornene functionalized to enable the formation of pectin hydrogels through photo-cross-linking in the presence of UV light, a bicysteine-modified peptide and a water-soluble photoinitiator (VA.086).[31] Albeit, this methodology is nontoxic and yielded a biodegradable and biocompatible hydrogel system; in the authors' opinion, the approach is significantly compromised by the high costs usually associated with norbornene click chemistry and the many chemical steps needed to go from the prepolymer stage to a hydrogel. Some recent studies have also demonstrated that pectin-based thin films and nanowires can be made from emulsion polymerization of glycidyl methacrylate-modified pectin.[51,75] In the present study, we have managed to convert methacrylate pectin into PEMA and have demonstrated that we could fine-tune its disintegration profile and mechanical properties by simply changing its methacrylation degree and the photoinitiator concentration. Notably, we have shown that we can cover a broad range of mechanical properties ranging from around 0.5 to 17 kPa through this methodology. Moreover, in contrast to alginate- and gelatin-based hydrogels, our hydrogel could endure cyclic loadings with a mechanical recovery close to 100%, which makes our system unique compared to many of the other available hydrogel-based systems out there. This attribute also makes the system amenable for skeletal tissue engineering as the ECM of skeletal tissues are exposed to dynamic loads on a daily basis.

The cell survival rate and the ability of cells to migrate, spread, differentiate, and connect with other cells are also imperative in tissue regeneration.[2] Even though our results with PEMA demonstrate a homogeneous distribution and a high viability of a wide range of cell types, PEMA did not facilitate sufficient cell−matrix interactions. This is not surprising, as most polysaccharide-based biomaterials are typically unable to induce strong cellular responses on their own.[25,72] Indeed, the native ECM comprises other bioactive molecules apart from polysaccharides, such as collagen fibers, fibronectin, laminin, and soluble growth factors.[25,52] We have tried to recapitulate this important feature into our system through gelatin incorporation. To this end, we have used thiolated gelatin as thiol groups can form covalent bonds with the acrylate groups on PEMA through a Michael addition reaction. This gelatin incorporation made the hydrogel system better suited for the survival and growth of adherent cells, as evidenced by the results obtained with the

DOI: 10.1021/acsami.9b00154
ACS Appl. Mater. Interfaces 2019, 11, 12283−12297

hMSCs. Specifically, they were shown to attach and spread into individual cells with well-defined actin stress fibers. Furthermore, the hMSCs could also secrete ALP and facilitate the formation of hydroxyapatite within the hydrogel matrix as is evident from XRD and FTIR spectroscopy, both of which are important hallmarks for osteogenic differentiation.

Advantageously, the methacrylate groups on PEMA allowed us to micropattern our cell-laden hydrogels through UV-assisted patterning. This unique feature can ultimately pave the road for the engineering of more complex and native-like tissues. We are aware of the fact that many groups have previously used GelMA and poly(ethylene glycol) diacrylate (PEGDA) for photopatterning cell-laden hydrogels. Even still, our new hydrogel solution displays some clear advantages over these state-of-the-art solutions.[71,76] We acknowledge that PEGDA is sufficiently stable; however, it is also bio-inert at the same time,[76] and therefore, does not exhibit cell spreading- and differentiation-inducing properties. Importantly, PEGDA is unable to promote cell migration and cell infiltration from the surrounding tissue, which in turn significantly limits its biointegration properties. While GelMA displays such properties, it rapidly degrades—both in vitro and in vivo—due to the action of the collagen-degrading protease, collagenase.[28,77] Another shortcoming of GelMA is intimately linked to their weak mechanical properties because they typically are not durable and tough enough for resisting the natural environment of load-bearing tissues.[28] We also note that most of the conventional hydrogel materials (not GelMA) are produced through complex multistep procedures that are costly and time-consuming. For instance, PEGDA, alginate, and hyaluronic acid-based hydrogels—the most commercially available ones—need some custom modification with either bioactive small peptides such as the arginine−glycine−aspartate (RGD) motif or proteins such as laminin and fibronectin. Even still, both solutions come at a high price, which significantly comprises the dream of custom-making tissue substitutes for the broad populace in an "off-the-shelf" manner.

PEMA-gelatin circumvents these shortcomings by providing a highly stable, mechanically durable, and tissue regenerative hydrogel without any unwanted tradeoffs. Since this system is based on readily available waste materials that are modified through simple one-step chemical protocols, this hydrogel is also easy to upscale and can be manufactured at a significantly lower price than other hydrogels currently in the market. Finally, the shear-thinning properties of PEMA make it amenable for 3D bioprinting and open up the possibility for launching cheaper bioinks.

CONCLUSIONS

Due to the aging population, tissue degeneration and organ failure are expected soon to become one of the biggest healthcare problems in the developed parts of the world. Albeit organ and tissue transplantation are viable options in many cases, the number of patients in need for transplantation by far outweighs the number of potential donors. Artificial tissues grown in the laboratory and targeted delivery of stem cells hold great promise for this problem, and could potentially meet this growing demand in the healthcare sector. The state-of-the-art methodology in the field is currently based on hydrogels that can stimulate and drive progenitor cells into new and healthy tissues. The critical importance of nontoxic, biocompatible, mechanically stable, tissue regenerative, as well as low-cost and scalable hydrogel systems has motivated researchers to search for abundant and bioactive polymers that can meet these requirements.

Here, we have joined this ongoing effort by transforming a naturally derived polymer, namely, pectin, into a cross-linkable hydrogel. The methodology that we employed to accomplish this was simply based on methacrylating pectin (PEMA) because we hypothesized that PEMA could form a hydrogel with low-level UV light and a photoinitiator. Indeed, this was the case, and to make the system more cell-friendly, we also incorporated gelatin into it. Our final hydrogel displayed an amazing portfolio of the highly sought properties in this field. This wide spectrum of properties includes mechanical toughness, load-bearing properties, bioactivity, stability in physiological environments, and nontoxicity, while the system all together remained less expensive and scalable. Notably, we have demonstrated that hMSCs growing inside such hydrogels can turn into bone cells and facilitate the formation of bonelike apatite, which is considered one of the hallmarks of bone differentiation. We have also demonstrated that our hydrogel could easily yield stable micropatterns with a 100 μm resolution and that hMSCs can grow within these (in a localized manner) and differentiate into bonelike cells. For these reasons, PEMA-gelatin holds great promise as a 3D biomaterial with intrinsic osteogenic activity of use for treating bone disorders. Overall, our data suggest that the PEMA-gelatin hydrogel can be used as a bone regenerative stem cell carrier as well as a biomaterial capable of driving stem cells into complex tissue-like architectures through UV micropatterning. The method presented here, therefore, presents a step forward in our capacity to stimulate stem cells to become mature tissues with the same complexity as native ones.

MATERIALS AND METHODS

Materials. Pectin from apple (50−75% esterification), 2-(*N*-morpholino)ethanesulfonic acid (MES), sodium chloride (NaCl), *N*-hydroxysuccinimide (NHS), 1-ethyl-3-(3-dimethylaminopropyl)-carbodiimide hydrochloride (EDC), 2-aminoethyl methacrylate hydrochloride (AEMA), 3-(trimethoxysilyl)propyl methacrylate (TPM), poly(2-hydroxyethyl methacrylate) (poly-HEMA), 2-hydroxy-4′-(2-hydroxyethoxy)-2-methylpropiophenone (Irgacure D-2959), deuterated water (D_2O), bovine serum albumin (BSA), β-glycerophosphate disodium salt hydrate, Dulbecco's phosphate-buffered saline (DPBS), Dulbecco's modified Eagle's medium (DMEM)-high glucose, penicillin−streptomycin, trypsin−ethylenediaminetetraacetic acid solution 1×, dexamethasone, and Alizarin Red S were purchased from Sigma-Aldrich (St. Louis, MO). Thiol-modified gelatin (Gelin-S) and degassed, deionized (DI) water at pH 5.0−8.0 (degassed (DG) water) were purchased from ESI-BIO. PC12 (ATCC CRL-1721) cell line, C2C12 (ATCC CRL-1772) cell line, and Roswell Park Memorial Institute (RPMI)-1640 culture medium (ATCC 30-2001) were purchased from LGC Standards, Sweden. Human bone marrow-derived mesenchymal stem cell (hMSC) (PT-2501) was obtained from Lonza Inc. Gibco. DMEM, low-glucose GlutaMAX supplement, pyruvate (catalog number: 21885025), snake skin dialysis tubing (3.5k molecular weight cut-off), 5-bromo-4-chloro-3-indolyl phosphate/nitroblue tetrazolium (BCIP/NBT), rhodamine phalloidin, Hoechst 33342, and alkaline phosphatase (ALP) substrate kit were purchased from Thermo Fisher Scientific. Fetal bovine serum (FBS) and fetal horse serum (FHS) were obtained from Biowest. Silicone Isolators (JTR24R-0.5) were purchased from Grace Bio-Labs, and 16% paraformaldehyde (formaldehyde) aqueous solution was obtained from electron microscopy sciences.

Synthesis of Pectin Methacrylate (PEMA). Pectin methacrylation was achieved by reacting pectin from apple peels (molar weight: ~706 kDa)[78] with AEMA. Briefly, to prepare the medium-PEMA with 48.82% theoretical methacrylation of acidic carboxyl groups, the pectin

DOI: 10.1021/acsami.9b00154
ACS Appl. Mater. Interfaces 2019, 11, 12283−12297

powder (1 g) was mixed at 1% (w/v) into a 50 mM MES buffer solution (100 mL, pH 6.5) containing 0.5 M NaCl at room temperature. After the powder was completely dissolved, 0.69 g (60 mM) of NHS and 2.3 g (120 mM) of EDC were added to this solution and stirred for 10 min to activate the carboxylic acid groups of the pectin. Then, 0.994 g (60 mM) of AEMA was added to the solution and allowed to react for 24 h at room temperature in the dark. The molar ratio of NHS/EDC/AEMA was maintained at 1:2:1. Low (30 mM) and high (90 mM) AEMA were used to synthesize low and high degrees of PEMA methacrylation, while keeping the NHS/EDC/AEMA molar ratio constant. After 24 h, the solution mixture was precipitated by the addition of excess acetone and dried under the fume hood. The resulting polymer was dehydrated and dissolved in 100 mL of deionized (DI) water for further purification and subsequently dialyzed against DI water for 3 days and lyophilized.

Preparation of Prepolymer Solution of PEMA-Gelin-S. 2% (w/v) lyophilized PEMA-Med was dissolved in DI water containing 0.6% (w/v) photoinitiator (Irgacure D-2959), and 2% (w/v) lyophilized Gelin-S was dissolved in degassed water (DG water). These solutions were mixed and vortexed together for 1 min. Therefore, the final concentration (w/v) of PEMA-Med and Gelin-S in prepolymer solution was always kept at 1% (w/v) containing 0.3% (w/v) photoinitiator.

Fabrication of Photo-Cross-Linked Hydrogels. To prepare photo-cross-linked PEMA (Low, Med, and High) hydrogels, 2% (w/v) freeze-dried PEMA polymer with different degrees of methacrylation was added and dissolved in a photoinitiator (PI) solution of 0.1 or 0.3% (w/v) in DI water at room temperature. Then, the PEMA polymer solutions were injected between a poly(methyl methacrylate) slide and a glass coverslip separated by a 2 mm spacer and then cross-linked using ultraviolet (UV) light ~7 mW/cm^2 for 1 min to form the hydrogels. This procedure was also used to form PEMA (Med)-Gelin-S hydrogel. All photo-cross-linked specimens were washed five times with DI water and then used for downstream studies.

Fourier Transform Infrared (FTIR) Spectroscopic Characterization. FTIR spectroscopy was used to observe the chemical composition and structural change both before and after UV curing of hydrogels. Therefore, a PerkinElmer Spectrum 100 FTIR spectrometer equipped with the attenuated total reflection accessory at a resolution of 4 cm^{-1} for 16 scans was used to record the FTIR spectra. The transmittance spectra for lyophilized PEMA (Low, Med, and High), Gelin-S, PEMA (Med)-Gelin-S, photo-cross-linked PEMA (Low, Med, and High), and photo-cross-linked PEMA (Med)-Gelin-S (N = 3) samples were collected after background subtraction at 25 °C in the range of 4000−500 cm^{-1}. PerkinElmer Spectrum software was used to correct baseline and normalize data. The FTIR spectrum of the photo-cross-linked PEMA (Med)-Gelin-S hydrogel indicates that the peaks related to acrylate and thiol groups completely disappeared, which shows that almost all of the thiol groups on Gelin-S reacted with the acrylate groups on PEMA.

Proton Nuclear Magnetic Resonance (^{1}H NMR) Characterization. The chemical modification of PEMA was quantified using ^{1}H NMR spectroscopy. The pectin powder and lyophilized PEMA (Low, Med, and High) (2% (w/v)) were mixed in D_2O and placed in NMR tubes to characterize the ^{1}H NMR spectroscopy. Moreover, the lyophilized PEMA (Low, Med, and High) (2% (w/v)) was dissolved in D_2O with 0.3% (w/v) PI, placed in NRM tubes, and photo-cross-linked by UV exposure ~7 mW/cm^2 for 1 min to form a hydrogel. D_2O was used as the solvent to dissolve the pectin samples due to their high affinity to water. The ^{1}H NMR spectra were recorded at room temperature on a Varian Mercury 400 MHz spectrometer by tetramethylsilane as internal standard. The conditions used for the experiments were spectral width 8012.82 Hz, acquisition time 8.18 s, and pulse 6.5 ms. All samples were obtained at room temperature. The chemical shifts (δ) were described in parts per million (ppm) related to the solvent's signal peak. Additionally, we estimated the degree of methacrylation from the relative integrated intensities of methyl protons (~1.9 ppm) in aminomethyl methacrylate and H-4 signal (~4.4 ppm) from the pectin molecule, and ~22, ~48, and ~61% degrees of methacrylation are obtained for low, medium, and high methacrylation, respectively.

ζ Potential Analysis. ζ potential of the pectin and PEMA (Low, Med, and High) prepolymer solutions were measured by laser Doppler anemometry using a Malvern Zetasizer instrument (Nano Series ZS, Malvern Instruments, Worcestershire, U.K.) fitted with a 4 mW He−Ne laser operating at a wavelength of 632.8 nm at 25 °C. Each specimen was dissolved in DI water at a concentration of 1 mg/mL.

Scanning Electron Microscopy (SEM). The microporous structure of samples was investigated using a scanning electron microscope (FEI Quanta 200 ESEM FEG), which was operated with an accelerating voltage of 10 kV. First, the photo-cross-linked hydrogel samples (N = 3 for each group) were washed, freeze-dried, cross-sectioned, and coated with gold (Au, 10 nm) prior to SEM imaging. Based on the captured SEM images, ImageJ software (National Institutes of Health (NIH)) was used to quantify of the pore size distribution.

Swelling and Disintegration Studies. The effect of the degree of methacrylation and photoinitiator concentration on the swelling behavior and stability of the photo-cross-linked pectin hydrogels was characterized by assessment of the hydration kinetics and dissolution behavior. To this end, to assess the swelling properties, PEMA hydrogels (N = 4 for each time point) were placed into six-well cell culture plates containing DPBS and then incubated at 37 °C to reach equilibrium swelling state. The DPBS was replaced every 2 days. At the respective time points, the swollen weight (W_s) of each hydrogel was recorded after being wiped by a paper wiper to drain the excess DPBS from the hydrogel surface. Afterward, the swollen hydrogels were freeze-dried to record their final dry weight (W_d). Using the following equation, the swelling ratio was calculated as the weight of the swollen hydrogel (W_s) to the weight of the freeze-dried sample (W_d).

$$\text{swelling ratio} = \frac{W_s - W_d}{W_d} \tag{1}$$

To evaluate the disintegration rate of the hydrogels, the final freeze-dried weight (W_f) and initial freeze-dried weight (W_I) of each sample were recorded at various time points. The disintegration rate was then obtained by dividing the final dry weight (W_f) by the initial dry weight (W_I) (eq 2). For each combination, at least four samples were analyzed.

$$\text{disintegration rate}(\%) = \left(\frac{W_f}{W_I} \times 100\right) - 100 \tag{2}$$

Rheology. The loss modulus (G'') and storage modulus (G') of PEMA solutions as well as PEMA-Gelin-S were tested by the Discovery Hybrid Rheometer HR-2 from TA Instruments with 40 mm diameter parallel plates at 25 °C. To determine the linear viscoelastic region, amplitude sweep was performed from 0.01 to 100 Pa at a fixed angular frequency of 1 rad/s. Moreover, steady shear experiments were performed to evaluate the shear thinning behavior of PEMA and PEMA-Gelin-S solutions at 25 °C. Flow sweep experiment with shear rate ranging from 0.01 to 100 s^{-1} was conducted, while the gap size was adjusted to 300 μm. All measurements were performed in triplicate.

Mechanical Characterization. To evaluate the effect of the degree of methacrylation, photoinitiator concentration, and Gelin-S on the mechanical behavior of the PEMA cross-linked hydrogels, compression and cyclic compression tests were performed at a constant compression rate of 0.5 mm/min using an Instron (model 5967, U.K.) mechanical tester with a 50 N load cell. Photo-cross-linked hydrogels disks (~10 mm diameter, ~2 mm thick, N = 6) were prepared and left to swell in DPBS at 37 °C overnight prior to mechanical testing. The hydrogels were compressed at a rate of 0.5 mm/min up to 80% strain. The compressive modulus of hydrogels was defined as the slope of stress vs. strain plots, corresponding to 15−25% strain. To determine the recovery of the samples, five complete compression recovery cycles up to 40% compressive strain were carried out at a loading rate of 0.5 mm/min. The recovery (%) was calculated as the ratio of toughness between fifth and second recovery cycles. The energy dissipation of hydrogels during cyclic loading was measured based on the area blocked within the loading and unloading hysteresis curves.

Cell Viability and Metabolic Activity of 3D Encapsulation of PC12, C2C12, and hMSCs. PC12 pheochromocytoma cell lines were

DOI: 10.1021/acsami.9b00154
ACS Appl. Mater. Interfaces 2019, 11, 12283−12297

cultured in RPMI-1640 medium supplemented with 10% (v/v) heat-inactivated FHS, 1% (v/v) penicillin−streptomycin, and 5% (v/v) FBS in T-75 flasks at 37 °C under a 5% CO_2 atmosphere. The PC12 cells were used at passage levels of 6−8 for all live-dead experiments. To evaluate the viability of 3D encapsulated PC12 cells, 1×10^6 cells/mL were encapsulated in prepolymer solutions containing 2% (w/v) PEMA (Low, Med, and High) in the presence of a 0.1% (w/v) or 0.3% (w/v) photoinitiator and then deposited (10 μL) into each microwell array (2 mm diameter × 1 mm depth) fixed on a glass slide. The solutions were cross-linked by photopolymerization under ∼7 mW/cm^2 UV for 1 min. The resulting samples were washed five times with DPBS to eliminate residual un-cross-linked reagents and cultured in PC12 cell growth medium (RPMI-1640 supplemented with heat-inactivated FHS (10% v/v), FBS (5% v/v), and penicillin−streptomycin (1% v/v)). Culture medium was changed every 2 days for 3 and 7 days. To assess the metabolic activity of 3D PC12 cell encapsulation, 3×10^6 cells/mL were used in the experiments.

Murine C2C12 myoblasts cells (between passages 6 and 8) were cultured in DMEM supplemented with FBS 10% (v/v), penicillin−streptomycin (1% v/v), and incubated at 37 °C and 5% CO_2. The cells were detached from flasks at 70% confluency by trypsinization, and they were either subcultured or used for experiments. For the cytotoxicity tests on 3D encapsulated C2C12 cells, aliquots of 1×10^6 cells/mL (for live/dead analysis) or 3×10^6 cells/mL (for metabolic activity monitoring) were encapsulated in prepolymer solutions containing 2% (w/v) PEMA (Low, Med, and High) in the presence of a 0.1% (w/v) or 0.3% (w/v) photoinitiator. The mixture of C2C12 cells and PEMA hydrogel precursor solution was deposited (10 μL) into each microwell array mounted on a glass slide and then photo-cross-linked under previously described UV conditions. The samples were washed five times with DPBS and then cultured in C2C12 growth media (DMEM supplemented with FBS 10% (v/v), penicillin−streptomycin (1% v/v)). The culture medium was replaced every 2 days for 3 and 7 days.

hMSCs were cultured in DMEM (low glucose, GlutaMAX) supplemented with FBS 10% (v/v) and 1% (v/v) penicillin−streptomycin. For osteogenic differentiation, the cells were cultured in DMEM (low glucose, GlutaMAX) containing 10% FBS, 1% (v/v) penicillin−streptomycin, 0.1 μm dexamethasone with 10 mM β-glycerophosphate, and 50 μg/mL ascorbic acid. hMSCs were used at passage numbers between 3 and 4 for all cell viability analysis and differentiation studies. 3×10^6 hMSCs/mL suspension was mixed with 2% (w/v) PEMA (Low, Med, and High) in the presence of a 0.1% (w/v) or 0.3% (w/v) photoinitiator and then deposited (10 μL) into each microwell array mounted on a glass slide and photo-cross-linked under previously described UV conditions. To encapsulate PEMA (Med)-Gelin-S-hMSC-laden hydrogels, 3% (w/v) PEMA (Med) and 1.2 mg of photoinitiator were dissolved in 133 μL of DPBS and Gelin-S (2% w/v) was dissolved in 200 μL of DG water separately, before mixing together. Afterward, 67 μL of hMSC solution with a density of 6×10^6 cells/mL was mixed with the hydrogel precursor and then deposited (10 μL) into each microwell array mounted on a glass slide. Finally, the PEMA (Med)-Gelin-S-hMSC-laden hydrogels were obtained through UV light-assisted cross-linking. All cell-encapsulated hydrogel samples were washed five times with DPBS and then cultured with either fresh hMSC growth media or differentiation media and incubated at 37 °C in a 5% CO_2 incubator. The culture media was replaced every 3 days up to 5 weeks. After 5 weeks, the cell-laden hydrogel samples were washed three times with DPBS and three times with sterile water and then lyophilized for analysis by XRD, EDAX, and FTIR techniques. The XRD analysis of the samples was achieved with a HUBER G670 X-ray powder diffractometer (Germany). An imaging plate detection method in the Guinier geometry equipped with a secondary monochrome and Cu X-ray tube with Cu Kα_1 radiation (λ = 1.54056 Å) was used to collect X-ray powder pattern. To this end, the X-ray generator tube was set to run at 40 kV and 40 mA at room temperature in the 2θ range of 3−80° and a scan step size of 0.005°. The EDAX analyses of the freeze-dried samples were performed by employing an energy-dispersive X-ray (EDX) spectroscopy (Oxford Instruments) detector, which was linked to the SEM (JSM-6010LA) instrument. The EDX permitted the quantitative determination of Ca and P, and the Ca/P ratio was measured by dividing the weight percentage of calcium element by the weight percentage of phosphorous element.

Microfabrication of Patterned PEMA (MED)-Gelin-S-hMSC-Laden Hydrogel. To prepare hMSC-encapsulated micropatterned hydrogel constructs, first the glass slides were cleaned via sonication in ethanol and deionized water several times and subsequently dried at room temperature. The glass slides were then soaked in 5% (v/v) TPM in toluene solution at 60 °C for at least 12 h, after which they were rinsed with ethanol and left to dry prior to coating them with poly-HMEA. Afterward, glass slides were treated with 4.5% (w/v) poly-HEMA solution in pure ethanol and left to dry for 3 days and sterilized by using UV light prior to use. Then, 150 μL of the prepared PEMA (Med)-Gelin-S-hMSC solution was pipetted between an untreated glass and coated glass slide separated by a 200 μm spacer. A photomask with parallel strips pattern (zebra pattern) with 100 μm width was placed on top of the glass slide and exposed to ∼7 mW/cm^2 UV for 1 min. Following polymerization, the coverslip was removed and washed five times with DPBS to remove unreacted solution and then cultured with either fresh hMSC growth media or differentiation media and incubated at 37 °C in a 5% CO_2 incubator. Here, the cell culture media was replaced every 3 days up to 2 weeks.

Live/Dead Viability Assay and Metabolic Activity Assay. Cell viabilities of hydrogel encapsulated PC12, C2C12, and hMSCs were evaluated by a live/dead assay kit (Life Technologies) following the suggested manufacturer's instructions. At predetermined time periods (days 1, 3, and 7), cell-encapsulated hydrogels were washed two times with DPBS and then stained with a live/dead assay kit containing calcein-AM (live cells) and ethidium homodimer-1 (dead cells) for 15 min at 37 °C. Cell-laden hydrogels were imaged by using a confocal laser scanning microscope (Zeiss LSM 700, Germany). The images were then assessed with ImageJ software (National Institutes of Health). To analyze the cell viability at the respective time points, the images were split into green (live cells) and red (dead cells) color channels to separately count live and dead cells. The cell viability percentage within the hydrogels was determined according to eq 3

$$\text{viability}(\%) = \frac{\text{live cell count}}{\text{total cell count}} \times 100 \tag{3}$$

Metabolic activity of hydrogel-encapsulated PC12, C2C12, and hMSCs were assessed by using a cell cytotoxicity assay kit (colorimetric) from Abcam following the manufacturer's instructions. First, the cell-laden hydrogels were washed twice with DPBS. Afterward, the hydrogels were transferred into 96-well plates containing 100 μL/well growth medium and 20 μL/well of assay solution and then incubated for 24 h at 37 °C. The optical densities of the respective samples were measured using a Spark multimode microplate reader (Tecan) at 570 and 605 nm. The ratio of OD_{570} to OD_{605} is used to determine the cell viability in each well. At least six samples were measured at each time point.

Quantification of Cell Spreading. Cell spreading within the micropatterned and unpatterned PEMA-Gelin-S-hMSC-laden hydrogels was evaluated via fluorescent staining. First, the samples were washed three times with DPBS and fixed using a solution of 4% paraformaldehyde in DPBS for 15 min at room temperature. Then, the samples were permeabilized for 5 min with 0.1% (w/v) Triton X-100 in DPBS at room temperature. A solution of 1% (w/v) BSA in DPBS was utilized to block the samples at room temperature for 30 min. Afterward, the samples were incubated for 45 min incubation at 37 °C with a solution of rhodamine phalloidin (1:40 dilution in 0.1% (w/v) BSA). The hydrogels were washed three times in DPBS and then the nuclei of the cells were stained with Hoechst (33342) and incubated for 15 min at 37 °C. The samples were then washed three times in DPBS and imaged using confocal laser scanning microscopy and finally evaluated with NIH ImageJ software. For each condition, at least six specimens were stained.

Alkaline Phosphatase (ALP) Staining. The intracellular alkaline phosphatase (ALP) activity of the micropatterned and unpatterned PEMA-Gelin-S-hMSC-laden hydrogels was evaluated by using a BCIP/NBT solution. First, the samples were washed three times in DPBS, then covered with BCIP/NBT, and finally left for 2 h at room temperature. In the end stage, the samples were rinsed three times in

DOI: 10.1021/acsami.9b00154
ACS Appl. Mater. Interfaces 2019, 11, 12283−12297

DPBS to eliminate excess BCIP/NBT assay before imaging with a Zeiss Axioscope 40 microscope (Carl Zeiss, Germany).

Alizarin Red S Staining. The PEMA-Gelin-S-hMSC-laden hydrogels were quantified by Alizarin Red S staining for mineralized bone nodule formation. To make the Alizarin Red S solution, 1 g of Alizarin Red S powder was dissolved in 50 mL of DPBS and then the pH of the solution was maintained at ∼4.2 to get a complete Alizarin Red S solution. Finally, the Alizarin Red S staining solution was filtered using a syringe filter (0.45 μm, Q-Max Syringe filter). The PEMA-Gelin-S-hMSC-laden hydrogels were first fixed with 4% formaldehyde solution at room temperature for 30 min. Then, the samples were washed with DPBS and immersed in the Alizarin Red S solution in the dark at room temperature. After 1 h, the samples were washed repeatedly with DPBS to remove the weakly adhered Alizarin Red S and then imaging was performed using a Zeiss Axioscope 40 microscope (Carl Zeiss, Germany).

Statistical Analysis. All statistical analysis was done using the GraphPad Prism software program (v7; San Diego). The significant differences among the grouped data sets (as in pore size analysis, viability, and cell coverage) were evaluated through one-way analysis of variance and followed by Tukey's post hoc test when the groups were independent and followed a normal distribution. If the data deviated from the normal, nonparametric Dunn's multiple comparison was used instead. Type 1 error rate was set to 0.05, and the statistical significance was specified as *($p < 0.05$), **($p < 0.01$), ***($p < 0.001$), ****($p < 0.0001$), and ns means not significant.

■ ASSOCIATED CONTENT

Supporting Information

The Supporting Information is available free of charge on the ACS Publications website at DOI: 10.1021/acsami.9b00154.

^{1}H NMR spectra and FTIR characterization, rheological analysis of PEMA-Gelin-S, mechanical analysis of PEMA-Gelin-S hydrogel, phalloidin-Hoechst nuclear staining staining of the PEMA-Gelin-S-hMSC-laden hydrogels at different time points and optical images of ALP expression of PEMA-Gelin-S-hMSC-laden hydrogels (PDF)

■ AUTHOR INFORMATION

Corresponding Author

*E-mail: aldo@nanotech.dtu.dk, alirezadolatshahipirouz@gmail.com.

ORCID

Cristian Pablo Pennisi: 0000-0002-7716-1182
Akhilesh K. Gaharwar: 0000-0002-0284-0201
Alireza Dolatshahi-Pirouz: 0000-0001-6326-0836

Notes

The authors declare no competing financial interest.

■ ACKNOWLEDGMENTS

A.D.-P. acknowledges the Danish Council for Independent Research (Technology and Production Sciences, 5054-00142B), Gigtforeningen (R139-A3864), and the Villum Foundation (10103). This work is also part of the VIDI research programme with project number R0004387, which is (partly) financed by the Netherlands Organisation for Scientific Research (NWO).

■ REFERENCES

(1) Spector, M. Biomedical Materials to Meet The Challenges of The Aging Epidemic. *Biomed. Mater.* **2018**, *13*, No. 030201.

(2) Madl, C. M.; Heilshorn, S. C.; Blau, H. M. Bioengineering Strategies to Accelerate Stem Cell Therapeutics. *Nature* **2018**, *557*, 335−342.

(3) Gaharwar, A. K.; Arpanaei, A.; Andresen, T. L.; Dolatshahi-Pirouz, A. 3D Biomaterial Microarrays for Regenerative Medicine: Current State-of-the-Art, Emerging Directions and Future Trends. *Adv. Mater.* **2016**, *28*, 771−781.

(4) Pedde, R. D.; Mirani, B.; Navaei, A.; Styan, T.; Wong, S.; Mehrali, M.; Thakur, A.; Mohtaram, N. K.; Bayati, A.; Dolatshahi-Pirouz, A.; et al. Emerging Biofabrication Strategies for Engineering Complex Tissue Constructs. *Adv. Mater.* **2017**, *29*, No. 1606061.

(5) Lei, Y. G.; Schaffer, D. V. A Fully Defined and Scalable 3d Culture System for Human Pluripotent Stem Cell Expansion and Differentiation. *Proc. Natl. Acad. Sci. U.S.A.* **2013**, *110*, E5039−E5048.

(6) Yuan, X. N.; Wei, Y. Y.; Villasante, A.; Ng, J. J. D.; Arkonac, D. E.; Chao, P. H. G.; Vunjak-Novakovic, G. Stem Cell Delivery in Tissue-Specific Hydrogel Enabled Meniscal Repair in an Orthotopic Rat Model. *Biomaterials* **2017**, *132*, 59−71.

(7) Madl, C. M.; LeSavage, B. L.; Dewi, R. E.; Dinh, C. B.; Stowers, R. S.; Khariton, M.; Lampe, K. J.; Nguyen, D.; Chaudhuri, O.; Enejder, A.; Heilshorn, S. C. Maintenance of Neural Progenitor Cell Stemness In 3d Hydrogels Requires Matrix Remodelling. *Nat. Mater.* **2017**, *16*, 1233−1242.

(8) Caliari, S. R.; Burdick, J. A. A practical guide to hydrogels for cell culture. *Nat. Methods* **2016**, *13*, 405−414.

(9) Agashi, K.; Chau, D. Y. S.; Shakesheff, K. M. The Effect of Delivery via Narrow-Bore Needles on Mesenchymal Cells. *Regener. Med.* **2009**, 49−64.

(10) Aguado, B. A.; Mulyasasmita, W.; Su, J.; Lampe, K. J.; Heilshorn, S. C. Improving Viability of Stem Cells During Syringe Needle Flow Through the Design of Hydrogel Cell Carriers. *Tissue Eng., Part A* **2012**, *18*, 806−815.

(11) Annabi, N.; Tamayol, A.; Uquillas, J. A.; Akbari, M.; Bertassoni, L. E.; Cha, C.; Camci-Unal, G.; Dokmeci, M. R.; Peppas, N. A.; Khademhosseini, A. 25th Anniversary Article: Rational Design and Applications of Hydrogels in Regenerative Medicine. *Adv. Mater.* **2014**, *26*, 85−124.

(12) Zhang, Y. S.; Khademhosseini, A. Advances in Engineering Hydrogels. *Science* **2017**, *356*, No. eaaf3627.

(13) Bao, M.; Xie, J.; Huck, W. T. S. Recent Advances in Engineering the Stem Cell Microniche in 3D. *Adv. Sci.* **2018**, *5*, No. 1800448.

(14) Mehrali, M.; Thakur, A.; Pennisi, C. P.; Talebian, S.; Arpanaei, A.; Nikkhah, M.; Dolatshahi-Pirouz, A. Nanoreinforced Hydrogels for Tissue Engineering: Biomaterials that are Compatible with Load-Bearing and Electroactive Tissues. *Adv. Mater.* **2017**, *29*, No. 1603612.

(15) Thakur, A.; Jaiswal, M. K.; Peak, C. W.; Carrow, J. K.; Gentry, J.; Dolatshahi-Pirouz, A.; Gaharwar, A. K. Injectable Shear-Thinning Nanoengineered Hydrogels for Stem Cell Delivery. *Nanoscale* **2016**, *8*, 12362−12372.

(16) Zhao, J. L.; Li, J. L.; Zhu, C. P.; Hu, F.; Wu, H. Y.; Man, X. H.; Li, Z. S.; Ye, C. Q.; Zou, D. W.; Wang, S. G. Design of Phase-Changeable and Injectable Alginate Hydrogel for Imaging-Guided Tumor Hyperthermia and Chemotherapy. *ACS Appl. Mater. Interfaces* **2018**, *10*, 3392−3404.

(17) Zhai, X. Y.; Ruan, C. S.; Ma, Y. F.; Cheng, D. L.; Wu, M. M.; Liu, W. G.; Zhao, X. L.; Pan, H. B.; Lu, W. W. 3D-Bioprinted Osteoblast-Laden Nanocomposite Hydrogel Constructs with Induced Microenvironments Promote Cell Viability, Differentiation, and Osteogenesis both In Vitro and In Vivo. *Adv. Sci.* **2018**, *5*, No. 1700550.

(18) Dolatshahi-Pirouz, A.; Nikkhah, M.; Gaharwar, A. K.; Hashmi, B.; Guermani, E.; Aliabadi, H.; Camci-Unal, G.; Ferrante, T.; Foss, M.; Ingber, D. E.; Khademhosseini, A. A Combinatorial Cell-Laden Gel Microarray for Inducing Osteogenic Differentiation of Human Mesenchymal Stem Cells. *Sci. Rep.* **2015**, *4*, No. 3896.

(19) Guermani, E.; Shaki, H.; Mohanty, S.; Mehrali, M.; Arpanaei, A.; Gaharwar, A. K.; Dolatshahi-Pirouz, A. Engineering Complex Tissue-Like Microgel Arrays for Evaluating Stem Cell Differentiation. *Sci. Rep.* **2016**, *6*, No. 30445.

(20) Hasany, M.; Thakur, A.; Taebnia, N.; Kadumudi, F. B.; Shahbazi, M.-A.; Pierchala, M. K.; Mohanty, S.; Orive, G.; Andresen, T. L.; Foldager, C. B.; et al. Combinatorial Screening of Nanoclay-Reinforced

DOI: 10.1021/acsami.9b00154
ACS Appl. Mater. Interfaces 2019, 11, 12283−12297

Hydrogels: A Glimpse of the "Holy Grail" in Orthopedic Stem Cell Therapy? *ACS Appl. Mater. Interfaces* **2018**, *10*, 34924−34941.
(21) Miao, T. X.; Wang, J. Q.; Zeng, Y.; Liu, G.; Chen, X. Y. Polysaccharide-Based Controlled Release Systems for Therapeutics Delivery and Tissue Engineering: From Bench to Bedside. *Adv. Sci.* **2018**, *5*, No. 1700513.
(22) Goh, M.; Kim, Y.; Gwon, K.; Min, K.; Hwang, Y.; Tae, G. In Situ Formation of Injectable and Porous Heparin-Based Hydrogel. *Carbohydr. Polym.* **2017**, *174*, 990−998.
(23) Lutolf, M. P.; Lauer-Fields, J. L.; Schmoekel, H. G.; Metters, A. T.; Weber, F. E.; Fields, G. B.; Hubbell, J. A. Synthetic Matrix Metalloproteinase-Sensitive Hydrogels for The Conduction Of Tissue Regeneration: Engineering Cell-Invasion Characteristics. *Proc. Natl. Acad. Sci. U.S.A.* **2003**, *100*, 5413−5418.
(24) Kloxin, A. M.; Kasko, A. M.; Salinas, C. N.; Anseth, K. S. Photodegradable Hydrogels for Dynamic Tuning of Physical and Chemical Properties. *Science* **2009**, *324*, 59−63.
(25) Yang, J. Z.; Zhang, Y. S.; Yue, K.; Khademhosseini, A. Cell-Laden Hydrogels for Osteochondral and Cartilage Tissue Engineering. *Acta Biomater.* **2017**, *57*, 1−25.
(26) Klotz, B. J.; Gawlitta, D.; Rosenberg, A.; Malda, J.; Melchels, F. P. W. Gelatin-Methacryloyl Hydrogels: Towards Biofabrication-Based Tissue Repair. *Trends Biotechnol.* **2016**, *34*, 394−407.
(27) Yu, F.; Han, X.; Zhang, K.; Dai, B.; Shen, S.; Gao, X.; Teng, H.; Wang, X.; Li, L.; Ju, H.; Wang, W.; Zhang, J.; Jiang, Q. Evaluation of A Polyvinyl Alcohol-Alginate Based Hydrogel for Precise 3d Bioprinting. *J. Biomed. Mater. Res., Part A* **2018**, *106*, 2944−2954.
(28) Jeon, O.; Shin, J.-Y.; Marks, R.; Hopkins, M.; Kim, T.-H.; Park, H.-H.; Alsberg, E. Highly Elastic and Tough Interpenetrating Polymer Network-Structured Hybrid Hydrogels for Cyclic Mechanical Loading-Enhanced Tissue Engineering. *Chem. Mater.* **2017**, *29*, 8425−8432.
(29) Munarin, F.; Guerreiro, S. G.; Grellier, M. A.; Tanzi, M. C.; Barbosa, M. A.; Petrini, P.; Granja, P. L. Pectin-Based Injectable Biomaterials for Bone Tissue Engineering. *Biomacromolecules* **2011**, *12*, 568−577.
(30) Munarin, F.; Tanzi, M. C.; Petrini, P. Advances in Biomedical Applications of Pectin Gels. *Int. J. Biol. Macromol.* **2012**, *51*, 681−689.
(31) Pereira, R. F.; Barrias, C. C.; Bartolo, P. J.; Granja, P. L. Cell-Instructive Pectin Hydrogels Crosslinked Via Thiol-Norbornene Photo-Click Chemistry for Skin Tissue Engineering. *Acta Biomater.* **2018**, *66*, 282−293.
(32) May, C. D. Industrial Pectins - Sources, Production and Applications. *Carbohydr. Polym.* **1990**, *12*, 79−99.
(33) Masmoudi, M.; Besbes, S.; Chaabouni, M.; Robert, C.; Paquot, M.; Blecker, C.; Attia, H. Optimization of Pectin Extraction from Lemon By-Product with Acidified Date Juice Using Response Surface Methodology. *Carbohydr. Polym.* **2008**, *74*, 185−192.
(34) Almeida, E. A. M. S.; Bellettini, I. C.; Garcia, F. P.; Farinácio, M. T.; Nakamura, C. V.; Rubira, A. F.; Martins, A. F.; Muniz, E. C. Curcumin-Loaded Dual Ph- And Thermo-Responsive Magnetic Microcarriers Based On Pectin Maleate For Drug Delivery. *Carbohydr. Polym.* **2017**, *171*, 259−266.
(35) Katav, T.; Liu, L.; Traitel, T.; Goldbart, R.; Wolfson, M.; Kost, J. Modified Pectin-Based Carrier for Gene Delivery: Cellular Barriers in Gene Delivery Course. *J. Controlled Release* **2008**, *130*, 183−191.
(36) Munarin, F.; Guerreiro, S. G.; Grellier, M. A.; Tanzi, M. C.; Barbosa, M. A.; Petrini, P.; Granja, P. L. Pectin-based injectable biomaterials for bone tissue engineering. *Biomacromolecules* **2011**, *12*, 568−577.
(37) Neves, S. C.; Gomes, D. B.; Sousa, A.; Bidarra, S. J.; Petrini, P.; Moroni, L.; Barrias, C. C.; Granja, P. L. Biofunctionalized Pectin Hydrogels as 3d Cellular Microenvironments. *J. Mater. Chem. A* **2015**, *3*, 2096−2108.
(38) Chen, F.; Ni, Y.; Liu, B.; Zhou, T.; Yu, C.; Su, Y.; Zhu, X.; Yu, X.; Zhou, Y. Self-Crosslinking and Injectable Hyaluronic Acid/Rgd-Functionalized Pectin Hydrogel for Cartilage Tissue Engineering. *Carbohydr. Polym.* **2017**, *166*, 31−44.
(39) Fares, M. M.; Sani, E. S.; Lara, R. P.; Oliveira, R. B.; Khademhosseini, A.; Annabi, N. Interpenetrating Network Gelatin Methacryloyl (Gelma) and Pectin-G-Pcl Hydrogels with Tunable Properties for Tissue Engineering. *Biomater. Sci.* **2018**, *6*, 2938−2950.
(40) Numata, K.; Yamazaki, S.; Katashima, T.; Chuah, J. A.; Naga, N.; Sakai, T. Silk-Pectin Hydrogel with Superior Mechanical Properties, Biodegradability, and Biocompatibility. *Macromol. Biosci.* **2014**, *14*, 799−806.
(41) Martins, J. G.; Camargo, S. E. A.; Bishop, T. T.; Popat, K. C.; Kipper, M. J.; Martins, A. F. Pectin-chitosan membrane scaffold imparts controlled stem cell adhesion and proliferation. *Carbohydr. Polym.* **2018**, *197*, 47−56.
(42) Jensen, T.; Dolatshahi-Pirouz, A.; Foss, M.; Baas, J.; Lovmand, J.; Duch, M.; Pedersen, F. S.; Kassem, M.; Bünger, C.; Søballe, K. Interaction of Human Mesenchymal Stem Cells with Osteopontin Coated Hydroxyapatite Surfaces. *Colloids Surf., B* **2010**, *75*, 186−193.
(43) Jensen, T.; Jakobsen, T.; Baas, J.; Nygaard, J. V.; Dolatshahi-Pirouz, A.; Hovgaard, M. B.; Foss, M.; Bünger, C.; Besenbacher, F.; Søballe, K. Hydroxyapatite Nanoparticles in Poly-D,L-Lactic Acid Coatings on Porous Titanium Implants Conducts Bone Formation. *J. Biomed. Mater. Res., Part A* **2010**, *95A*, 665−672.
(44) Kim, H. D.; Lee, E. A.; An, Y. H.; Kim, S. L.; Lee, S. S.; Yu, S. J.; Jang, H. L.; Nam, K. T.; Im, S. G.; Hwang, N. S. Chondroitin Sulfate-Based Biomineralizing Surface Hydrogels for Bone Tissue Engineering. *ACS Appl. Mater. Interfaces* **2017**, *9*, 21639−21650.
(45) Thorpe, A. A.; Creasey, S.; Sammon, C.; Le Maitre, C. L. Hydroxyapatite Nanoparticle Injectable Hydrogel Scaffold to Support Osteogenic Differentiation of Human Mesenchymal Stem Cells. *Eur. Cells Mater.* **2016**, *32*, 1−23.
(46) Vo, T. N.; Shah, S. R.; Lu, S.; Tatara, A. M.; Lee, E. J.; Roh, T. T.; Tabata, Y.; Mikos, A. G. Injectable Dual-Gelling Cell-Laden Composite Hydrogels for Bone Tissue Engineering. *Biomaterials* **2016**, *83*, 1−11.
(47) Kadri, R.; Ben Messaoud, G.; Tamayol, A.; Aliakbarian, B.; Zhang, H. Y.; Hasan, M.; Sanchez-Gonzalez, L.; Arab-Tehrany, E. Preparation and characterization of nanofunctionalized alginate/methacrylated gelatin hybrid hydrogels. *RSC Adv.* **2016**, *6*, 27879−27884.
(48) Winning, H.; Viereck, N.; Nørgaard, L.; Larsen, J.; Engelsen, S. B. Quantification of The Degree of Blockiness in Pectins Using 1h NMR Spectroscopy and Chemometrics. *Food Hydrocolloids* **2007**, *21*, 256−266.
(49) Grassino, A. N.; Brnčić, M.; Vikić-Topić, D.; Roca, S.; Dent, M.; Brnčić, S. R. Ultrasound Assisted Extraction and Characterization of Pectin from Tomato Waste. *Food Chem.* **2016**, *198*, 93−100.
(50) Eke, G.; Mangir, N.; Hasirci, N.; MacNeil, S.; Hasirci, V. Development of A UV Crosslinked Biodegradable Hydrogel Containing Adipose Derived Stem Cells to Promote Vascularization for Skin Wounds and Tissue Engineering. *Biomaterials* **2017**, *129*, 188−198.
(51) Kollarigowda, R. H. Novel Polysaccharide Nanowires; Synthesized from Pectin-Modified Methacrylate. *RSC Adv.* **2015**, *5*, 102143−102146.
(52) Jeon, O.; Bouhadir, K. H.; Mansour, J. M.; Alsberg, E. Photocrosslinked Alginate Hydrogels with Tunable Biodegradation Rates and Mechanical Properties. *Biomaterials* **2009**, *30*, 2724−2734.
(53) Lima, A. C.; Song, W.; Blanco-Fernandez, B.; Alvarez-Lorenzo, C.; Mano, J. F. Synthesis of Temperature-Responsive Dextran-MA/PNIPAAm Particles for Controlled Drug Delivery Using Superhydrophobic Surfaces. *Pharm. Res.* **2011**, *28*, 1294−1305.
(54) Zhao, C.; Shi, Q.; Hou, J.; Xin, Z.; Jin, J.; Li, C.; Wong, S.-C.; Yin, J. Capturing Red Blood Cells from the Blood by Lectin Recognition on a Glycopolymer-Patterned Surface. *J. Mater. Chem. A* **2016**, *4*, 4130−4137.
(55) Konuray, O.; Fernández-Francos, X.; Ramis, X.; Serra, À. New Allyl-Functional Catalytic Comonomers for Sequential Thiol-Michael and Radical Thiol-Ene Reactions. *Polymer* **2018**, *138*, 369−377.
(56) Suo, H.; Zhang, D.; Yin, J.; Qian, J.; Wu, Z. L.; Fu, J. Interpenetrating Polymer Network Hydrogels Composed of Chitosan and Photocrosslinkable Gelatin with Enhanced Mechanical Properties for Tissue Engineering. *Mater. Sci. Eng., C* **2018**, 612−620.
(57) Saraiva, S. M.; Miguel, S. P.; Ribeiro, M. P.; Coutinho, P.; Correia, I. J. Synthesis and Characterization of A Photocrosslinkable

DOI: 10.1021/acsami.9b00154
ACS Appl. Mater. Interfaces 2019, 11, 12283−12297

Chitosan−Gelatin Hydrogel Aimed for Tissue Regeneration. *RSC Adv.* **2015**, *5*, 63478−63488.
(58) Annabi, N.; Nichol, J. W.; Zhong, X.; Ji, C. D.; Koshy, S.; Khademhosseini, A.; Dehghani, F. Controlling the Porosity and Microarchitecture of Hydrogels for Tissue Engineering. *Tissue Eng., Part B* **2010**, *16*, 371−383.
(59) Karageorgiou, V.; Kaplan, D. Porosity of 3d Biomaterial Scaffolds and Osteogenesis. *Biomaterials* **2005**, *26*, 5474−5491.
(60) Engler, A. J.; Sen, S.; Sweeney, H. L.; Discher, D. E. Matrix Elasticity Directs Stem Cell Lineage Specification. *Cell* **2006**, *126*, 677−689.
(61) Huebsch, N.; Lippens, E.; Lee, K.; Mehta, M.; Koshy, S. T.; Darnell, M. C.; Desai, R. M.; Madl, C. M.; Xu, M.; Zhao, X.; et al. Matrix Elasticity of Void-Forming Hydrogels Controls Transplanted-Stem-Cell-Mediated Bone Formation. *Nat. Mater.* **2015**, *14*, 1269.
(62) Yue, K.; Trujillo-de Santiago, G.; Alvarez, M. M.; Tamayol, A.; Annabi, N.; Khademhosseini, A. Synthesis, properties, and biomedical applications of gelatin methacryloyl (GelMA) hydrogels. *Biomaterials* **2015**, *73*, 254−271.
(63) Meinert, C.; Schrobback, K.; Levett, P. A.; Lutton, C.; Sah, R. L.; Klein, T. J. Tailoring hydrogel surface properties to modulate cellular response to shear loading. *Acta Biomater.* **2017**, *52*, 105−117.
(64) U.S. Food and Drug Administration. *Guidance for Industry. Biologics License Applications for Minimally Manipulated Unrelated Allogeneic Placenta/Umbilical Cord Blood Intended for Hematopoietic and Immunologic Reconstitution in Patients with Disorders Affecting the Hematopoietic System*; U.S. Department of Health and Human Services, FDA, 2014.
(65) Rehfeldt, F.; Brown, A. E. X.; Raab, M.; Cai, S.; Zajac, A. L.; Zemel, A.; Discher, D. E. Hyaluronic Acid Matrices Show Matrix Stiffness in 2d And 3d Dictates Cytoskeletal Order and Myosin-Ii Phosphorylation within Stem Cells. *Integr. Biol.* **2012**, *4*, 422−430.
(66) Golub, E. E.; Boesze-Battaglia, K. The Role of Alkaline Phosphatase in Mineralization. *Curr. Opin. Orthop.* **2007**, *18*, 444−448.
(67) Chen, W.; Long, T.; Guo, Y.-J.; Zhu, Z.-A.; Guo, Y.-P. Hydrothermal Synthesis of Hydroxyapatite Coatings with Oriented Nanorod Arrays. *RSC Adv.* **2014**, *4*, 185−191.
(68) Shahabi, S.; Najafi, F.; Majdabadi, A.; Hooshmand, T.; Haghbin Nazarpak, M.; Karimi, B.; Fatemi, S. M. Effect of Gamma Irradiation on Structural and Biological Properties of A Plga-Peg-Hydroxyapatite Composite. *Sci. World J.* **2014**, *2014*, No. 420616.
(69) Aubin, H.; Nichol, J. W.; Hutson, C. B.; Bae, H.; Sieminski, A. L.; Cropek, D. M.; Akhyari, P.; Khademhosseini, A. Directed 3d Cell Alignment and Elongation in Microengineered Hydrogels. *Biomaterials* **2010**, *31*, 6941−6951.
(70) Nikkhah, M.; Eshak, N.; Zorlutuna, P.; Annabi, N.; Castello, M.; Kim, K.; Dolatshahi-Pirouz, A.; Edalat, F.; Bae, H.; Yang, Y.; Khademhosseini, A. Directed Endothelial Cell Morphogenesis in Micropatterned Gelatin Methacrylate Hydrogels. *Biomaterials* **2012**, *33*, 9009−9018.
(71) Jana, S.; Levengood, S. K. L.; Zhang, M. Q. Anisotropic Materials for Skeletal-Muscle-Tissue Engineering. *Adv. Mater.* **2016**, *28*, 10588−10612.
(72) Diekjürgen, D.; Grainger, D. W. Polysaccharide Matrices Used in 3d in Vitro Cell Culture Systems. *Biomaterials* **2017**, *141*, 96−115.
(73) Coimbra, P.; Ferreira, P.; de Sousa, H. C.; Batista, P.; Rodrigues, M. A.; Correia, I. J.; Gil, M. H. Preparation and Chemical and Biological Characterization of A Pectin/Chitosan Polyelectrolyte Complex Scaffold for Possible Bone Tissue Engineering Applications. *Int. J. Biol. Macromol.* **2011**, *48*, 112−118.
(74) Tentor, F. R.; de Oliveira, J. H.; Scariot, D. B.; Lazarin-Bidoia, D.; Bonafe, E. G.; Nakamura, C. V.; Venter, S. A. S.; Monteiro, J. P.; Muniz, E. C.; Martins, A. F. Scaffolds Based on Chitosan/Pectin Thermosensitive Hydrogels Containing Gold Nanoparticles. *Int. J. Biol. Macromol.* **2017**, *102*, 1186−1194.
(75) Villanova, J. C. O.; Ayres, E.; Oréfice, R. L. Design, Characterization and Preliminary in Vitro Evaluation of A Mucoadhesive Polymer Based on Modified Pectin and Acrylic Monomers with Potential Use as A Pharmaceutical Excipient. *Carbohydr. Polym.* **2015**, *121*, 372−381.
(76) Occhetta, P.; Sadr, N.; Piraino, F.; Redaelli, A.; Moretti, M.; Rasponi, M. Fabrication of 3d Cell-Laden Hydrogel Microstructures Through Photo-Mold Patterning. *Biofabrication* **2013**, *5*, No. 035002.
(77) Fathi, A.; Lee, S.; Breen, A.; Shirazi, A. N.; Valtchev, P.; Dehghani, F. Enhancing the Mechanical Properties and Physical Stability of Biomimetic Polymer Hydrogels for Micro-Patterning and Tissue Engineering Applications. *Eur. Polym. J.* **2014**, *59*, 161−170.
(78) Zhang, L. F.; Ye, X. Q.; Ding, T.; Sun, X. Y.; Xu, Y. T.; Liu, D. H. Ultrasound effects on the degradation kinetics, structure and rheological properties of apple pectin. *Ultrason. Sonochem.* **2013**, *20*, 222−231.

DOI: 10.1021/acsami.9b00154
ACS Appl. Mater. Interfaces 2019, 11, 12283−12297